Simvastatin Therapy Attenuates Memory Deficits that Associate to Brain Monocyte Infiltration in Chronic Hypercholesterolemic ApoE$^{-/-}$ Mice

Short running title: Monocytes and memory deficits in hypercholesterolemia.

Nicholas Don-Doncow[a,b], Frank Matthes[a,b], Hana Matuskova[a,b,c,d], Sara Rattik[e], Lotte Vanherle[a,b], Sine Kragh Petersen[f], Anetta Härtlova[f] & Anja Meissner[a,b,d]

[a] Department of Experimental Medical Sciences, Lund University, Sweden

[b] Wallenberg Centre for Molecular Medicine, Lund University, Sweden

[c] Department of Neurology, University Hospital Bonn, Germany

[d] German Center for Neurodegenerative Diseases, Bonn, Germany

[e] Department of Clinical Science, Lund University, Sweden

[f] Department of Microbiology and Immunology, Wallenberg Centre for Molecular and Translational Medicine, University of Gothenburg, Sweden

Correspondence to: Anja Meissner; Klinikgatan 32, SE-22184 Lund, Sweden; anja.meissner@med.lu.se; +46 (0)46 22 20641

Manuscript category: Original Article

Word count: 4729

Abstract

Aims: Metabolic and cardiovascular disease is the most prevalent disease burden in the developed world and risk factor for progressive cognitive decline. Evidence associates cardiovascular risk factors to unfavorable systemic and neuro-inflammation and to cognitive decline. Cardiovascular therapeutics (e.g., statins and anti-hypertensive drugs) possess immune-modulatory functions in parallel to their principle cholesterol- or blood pressure (BP)-lowering properties. How their ability to modify immune responses affects cognitive function is unknown.

Methods and Results: By using flow cytometry, Elisa, qPCR, Western blotting and object recognition tasks, we examined the effect of chronic hypercholesterolemia on inflammation and memory function in Apolipoprotein E (ApoE) knockout mice and normocholesterolemic wild-type (WT) mice. Chronic hypercholesterolemia associated to moderate BP elevations and apparent immune system activation characterized by higher proportions of circulating pro-inflammatory Ly6Chi monocytes in aged ApoE$^{-/-}$ mice. The persistent low-grade immune activation associated to chronically elevated cholesterol levels facilitates the infiltration of pro-inflammatory Ly6Chi monocytes into the brain of aged ApoE$^{-/-}$ but not WT mice, potentially promoting the development of memory dysfunction associated to chronic hypercholesterolemia. Therapeutic administration of the cholesterol-lowering drug simvastatin significantly reduced BP, systemic and neuro-inflammation, and the occurrence of memory deficits in aged ApoE$^{-/-}$ mice. BP-lowering therapy alone (i.e. hydralazine) attenuated some neuro-inflammatory signatures but not the occurrence of memory deficits. When administered in combination, it reduced effectiveness of statin therapy in some instances.

Conclusion: Our study suggests a causative link between chronic hypercholesterolemia, myeloid cell activation and neuro-inflammation with memory impairment. Cholesterol-lowering therapy provides effectiveness to

attenuate memory impairment and inflammatory events and hence, emerges as safe therapeutic strategy to control hypercholesterolemia-associated memory decline. Moreover, our results support the notion that chronic rather than late-life exposure to cardiovascular risk factors contributes to the development of cognitive dysfunction in the elderly.

Translational Perspective: Our study links chronic hypercholesterolemia in mice to specific immune responses that may underlie the development of memory impairment. We describe favorable outcomes in respect to neuro-inflammation and memory function in chronically hypercholesterolemic mice after statin therapy. Thus, our study (**1**) could open the door for available cardiovascular disease (CVD) therapeutics with long-term safety profiles to managing cognitive dysfunction in patients suffering from CVD, and (**2**) stimulate targeted monitoring of the inflammatory signature in patients with high cardiovascular burden since it could be a surrogate biomarker of cognitive decline.

Keywords: chronic hypercholesterolemia, immune activation, pro-inflammatory monocytes, neuro-inflammation, memory impairment

Introduction:

Cognitive decline is an increasingly common problem that progresses with age. By gradually interfering with daily functioning and well-being, it poses an enormous burden on affected people and their environment.[1, 2] In recent years, the apparent role of cardiovascular risk factors as important modifiable elements in the development of cognitive decline has become subject of clinical as well as pre-clinical research efforts.[2-4] Over the past two decades, evidence accumulated suggesting a prominent link between mid-life chronic hypercholesterolemia and/or hypertension and the development of dementia later in life.[5, 6] As a consequence, the management of cardiovascular risk factors not only serves to preventing often detrimental acute consequences of for instance, hypertension or dyslipidemia but also to minimize potential adverse cognitive outcomes later on. A number of observational and randomized studies reported beneficial effects of antihypertensive therapies on cognitive outcome.[7-9] Nonetheless, existing distinctions regarding effectiveness between different classes of hypertension medication have been shown,[7] and longitudinal studies suggested risk-reducing effects of anti-hypertensive treatment rather than an efficacy to slowing or treating manifested hypertension-associated cognitive impairment.[10] Likewise, the use of statins in controlling risk factors for dementia prevention or treatment is controversially discussed. Their therapeutic efficacy that initially emerged from findings showing its positive effects on various factors related to memory function,[11, 12] such as brain derived neurotrophic growth factor (BDNF)[13, 14] was increasingly argued as case studies raised concerns regarding a contributory role of statins in development of cognitive problems.[15, 16] Due to the discrepancies observed between studies and the lack of knowledge regarding underlying mechanisms, strategies to combat cognitive impairment resulting from cardiovascular risk factors or cardiovascular disease (CVD) are yet to be established.

Immune system alterations and inflammation are not only hallmarks of many CVDs and their risk factors but have increasingly been recognized as contributors to impaired cognitive function in older people.[17-19] Pharmaceuticals directed against inflammation evidently improve cognitive alterations associated to normal aging, CVDs, and classical neurodegenerative diseases.[20, 21] Moreover, multiple drugs commonly used in the cardiovascular field possess immune-modulatory actions in parallel to their principle cholesterol- or blood pressure (BP)-lowering effects.[22, 23] How this ability of CVD therapeutics to modify immune responses affects cognitive function is unknown. One of the bottlenecks hampering the targeted use of CVD therapeutics as approach to minimize CVD-associated cognitive impairment is the lacking understanding of specific inflammatory signatures that relate to cognitive impairment in patients with increased cardiovascular burden.

The herein presented study investigated the effect of chronic exposure to elevated plasma cholesterol levels on systemic and neuro-inflammation and memory function in ageing mice. Using mice deficient in

Apolipoprotein E (ApoE), which normally facilitates cholesterol clearance in the liver and thus, controls plasma cholesterol levels, allowed us to mimic a chronically hypercholesterolemic state under normal dietary conditions. To study the effect of chronic hypercholesterolemia on systemic and neuro-inflammation and memory performance, we compared ApoE$^{-/-}$ mice to normocholesterolemic WT mice. The ApoE$^{-/-}$ model presents with evident structural and functional vascular alterations that extend to the cerebral arteriole tree.[24] Besides, an age-related neurodegeneration of currently unknown cause has been described in these mice[25] and recent studies provided insight into the role of ApoE-deficiency in cognitive performance[26] and inflammation.[27] Here, we tested the efficacy of CVD therapeutics as treatment for memory impairment associated to the increased cardiovascular burden in aged ApoE$^{-/-}$ mice (i.e. increased plasma cholesterol and higher-than-normal BP). To this end, we therapeutically administered the statin simvastatin that has been attributed a strong anti-inflammatory character by regulating proliferation and activation of macrophages,[29, 30] and/or the smooth muscle relaxant agent hydralazine, known to reduce leukocyte migration in spontaneously hypertensive rats.[28] Our findings provide evidence that early life exposure to high cholesterol rather than increases in plasma cholesterol and BP later in life negatively affect memory performance. We underscore a causative role of myeloid cell activation in the development of neuro-inflammation associated to chronic hypercholesterolemia as well as cell type-specific drug effects that may limit their efficacy.

Material and Methods:

An expanded Methods section is available in the online Data Supplement.

Materials: All chemical reagents and solutions were purchased from Fisher Scientific (Göteborg, Sweden), Saveen & Werner (Limhamn, Sweden) or Sigma-Aldrich (Stockholm, Sweden) unless otherwise stated. Commercially available primary antibodies against CD3 (Bio-techne, UK), PSD-95, SNAP-25, NeuN and BDNF (Abcam, UK), CD68 (Invitrogen, Sweden) and Iba-1 (Wako, Japan) were used for immunofluorescence. Secondary antibodies Alexa Fluor 488 donkey anti-mouse, anti-rabbit, goat anti-rabbit or goat anti-rat Fluor 594 (Nordic Biosite, Sweden) were used for visualization. Primers for qPCR were purchased from Eurofins (Ebersberg, Germany).

Animals: This investigation conforms to the Guide for Care and Use of Laboratory Animals published by the European Union (**Directive 2010/63/EU**) and with the ARRIVE guidelines. All animal care and experimental protocols were approved by the institutional animal ethics committees at the University of Barcelona (CEEA) and Lund University (5.8.18-12657/2017) and conducted in accordance with European animal protection laws.
Male wild-type (WT) C57Bl/6J mice and Apolipoprotein E knockout (ApoE$^{-/-}$) mice (B6.129P2-Apoe (tm1Unc)/J) were obtained from Jackson Laboratories and bred in a conventional animal facility under standard conditions with a 12h:12h light-dark cycle, and access to food (standard rodent diet) and water *ad libitum*. Mice with a body weight BW $\geq$ 25g were housed in groups of 4-5 in conventional transparent polycarbonate cages with filter tops. ApoE$^{-/-}$ and C57Bl/6J (WT) mice at the age of 4 and 12 months (N=10 per group) were used to assess the effect of ageing on inflammatory status and brain phenotype (Fig.1A). At the age of 12 months, another group of ApoE$^{-/-}$ mice was randomly assigned to the following experimental groups using the computer software *Research Randomizer* (http://www.randomizer.org/): aged control, aged + hydralazine (25 mg/L), aged + simvastatin (2.5 mg/L), and aged + hydralazine/simvastatin combination (N=10 for simvastatin and hydralazine treatment; N=8 for combination treatment). The calculated doses given to the mice were 5 mg/kg/d for hydralazine and 0.5 mg/kg/d for simvastatin, which corresponds to 10 mg/kg/d and 20 mg/kg/d in humans, respectively (allometric scaling was used to convert doses amongst species[31]). Treatment was administered via drinking water over a course of two months. The mice in this experimental cohort were 14 months of age at time of sacrifice (Fig.1B). ApoE$^{-/-}$ mice at the age of 4 months were used as young controls (N=10). To ensure blinding experiments were performed after the animals and samples had received codes that did not reveal the identity of the treatment. In order to obey the rules for animal welfare, we designed experimental groups in a way that minimizes stress for the animals and guarantees maximal information using the lowest group size possible when calculated with a type I error rate of $\alpha = 0.05$ (5%) and Power of $1-\beta > 0.8$ (80%) based on

preliminary experiments. At termination, brain tissue was distributed to the different experiments as follows: Young (4 months) and aged (12 months) WT and ApoE$^{-/-}$ mice (N=10 each) for flow cytometric assessment of one hemisphere, N=5 each for cortex and hippocampus fractionation of one hemisphere and N=5 for whole hemisphere RNA and protein isolation (Fig.1A). Young (4 months), aged (14 months), hydralazine- and simvastatin treated (N=5 each) and combination-treated (N=3) ApoE$^{-/-}$ mice for whole brain cryo-sectioning, cortex and hippocampus fractionation of one hemisphere (N=5 each) as well as one hemisphere (N=5 each) for whole hemisphere RNA and protein isolation (Fig.1B).

Open Field testing: To test novel environment exploration, general locomotor activity, and screen for anxiety-related behavior mice were subjected to an open field exploration task using a video tracking system and the computer software EthoVision XT® (Noldus Information Technology, Netherlands) as described before.[20] Mice were placed individually into an arena (56 × 56 cm), which was divided into a grid of equally sized areas. The software recorded each line crossing as one unit of exploratory activity. The following behavioral parameters were measured: activity, active time, mobile time, slow activity, mobile counts, and slow mobile counts.

Novel object recognition (NOR): As previously described,[3, 20, 32] a NOR task was employed to assess non-spatial memory components. Briefly, mice were habituated to the testing arena for 10 minutes over a period of 3 days. On test day, each mouse was exposed to two objects for 10 minutes. 5 min or 24 hrs later, mice were re-exposed to one object from the original test pair and to a novel object. The movements of the animal were video tracked with the computer software EthoVision XT® (Noldus Information Technology, Netherlands). A delay interval of 5 minutes was chosen to test short-term retention of object familiarity, and with a delay interval longer of 24 hrs, we tested long-term hippocampus-dependent memory function.[3, 33] A recognition index (RI) as the main index of retention was calculated by the time spent investigating the novel object relative to the total object investigation [$RI = T_{Novel}/(T_{Novel} + T_{Familiar})$]. RI=0.5 indicates no preference for neither familiar nor novel object. Mice with total object exploration times ($T_{Novel} + T_{Familiar}$) below 20s were excluded from the analysis.

Object placement task: To test spatial recognition memory, mice were placed individually into an arena (56 × 56 cm). Each mouse was exposed to two objects for 10 minutes. 5 min later, mice were re-exposed to both objects, of which one remained in the original place and the second object was moved to a novel place. Exploration of the objects was assessed manually with a stopwatch when mice sniffed, whisked, or looked at the objects from no more than 1 cm away. The time spent exploring the objects in new (novel) and old (familiar) locations was recorded during 5 min. A location index was calculated $RI = T_{Novel}/(T_{Novel} + T_{Familiar})$, where T_{novel} is the time spent exploring the displaced object and $T_{familiar}$ is the time spent exploring the non-displaced object. RI=0.5 indicates no preference for neither familiar nor novel object. Mice with total object exploration times ($T_{Novel} + T_{Familiar}$) below 20s were excluded from the analysis.

Blood pressure measurements: BP was measured in conscious mice using tail-cuff plethysmography (Kent Scientific, CODA, UK). After a one-week handling period, mice were acclimatized to the restrainers and the tail cuff for a training period of 7 days. Mice were trained to walk into the restrainers and the holders were adjusted to limit the amount of movement. During this training period, first BP measurement were performed to familiarize the animals with the experimental procedure (e.g., cuff inflation). BP measurements were conducted in a designated quiet area where the mice were protected from direct light. Before and during each measurement, mice are placed on a heating pad kept at 35°C. Actual BP measurements commenced after the training week. Data were recorded once mice presented with stable readings over the course of one week. During BP measurements, 30 inflation cycles were recorded of which the first 14 were regarded as acclimatization cycles and only cycles 15-30 were included in the analyses. BP was assessed at the age of 4 and 12 months in ApoE$^{-/-}$ and WT mice (Fig.1A). In aged ApoE$^{-/-}$ mice that received treatment, BP was longitudinally assessed at experiment start (12 months) and after 8 weeks of treatment (14 months; Fig.1B).

Fluorescence activated cell sorting: Before euthanasia through cervical dislocation, mice were sedated using inhalation anesthesia (isofluorane 2.5% at 1.5L/min in room air) for whole blood collection. Whole blood was collected in EDTA-coated tubes and red blood cells were lysed before samples were incubated in F_c block solution; FACS buffer (PBS + 2 % FBS + 2 mM EDTA; pH 7.4) + anti-CD16/CD32, for 15 minutes followed by primary antibodies for 30 minutes at 4^oC. After centrifugation, the supernatant was decanted, washed, and pellets were re-suspended in FACS buffer. Brain tissue was enzymatically digested and homogenized. After density separation using Percoll (GE Healthcare), pellets were reconstituted in F_c block and incubated for 15 minutes prior to staining with antibodies for 30 min (see data supplement for detailed list of antibodies). Data acquisition was carried out in a BD LSR Fortessa cytometer using FacsDiva software Vision 8.0 (BD Biosciences). Data analysis was performed with FlowJo software (version 10, TreeStar Inc., USA). Cells were plotted on forward versus side scatter and single cells were gated on FSC-A versus FSC-H linearity.

Brain macrophage analysis: Coronal brain sections (10μm thickness) of each experimental group were immune-stained with Iba1 (WAKO, Japan) and CD68 (Invitrogen, Sweden). The total number of Iba1+ cells was counted in two regions of the hippocampus (dentate gyrus; DG and the cornu ammonis 1; CA1) in each hemisphere and in five regions of interests (ROIs) of the cortex using a fluorescence microscope (Axio Imager .M2, Zeiss). The cells were classified into three activation state groups based on morphology where *Ramified* (resting state) denotes Iba-1+ cells with a small cell body and extensive branched processes, *Intermediate* denotes Iba-1+ cells with enlarged cell body and thickened, reduced branches not longer than twice the cell body length and *Round* (active state) denotes Iba-1+ cells with round cell body without visible branches. In all sections, the total numbers of CD68+ Iba1+ cells were recorded.

Cell culture: Bone-marrow-derived macrophages (BMDMs) were generated by culturing freshly isolated mouse bone marrow cells from C57BL/6J mice in IMDM medium (GIBCO, Life Technologies) supplemented with 10% FCS (GIBCO, Life Technologies), 100 U/ml penicillin (Sigma-Aldrich), and 100 U/ml streptomycin (Sigma-Aldrich), 2 mM glutamine (Sigma-Aldrich) and 20% (v/v) L929 conditional medium for 7 days. Human monocytic THP-1 cells (ATCC #TIB-202) were cultured in RPMI-1640 containing 10% fetal bovine serum, 0.05 mM β-mercaptoethanol, and 1 % penicillin-streptomycin in large culture flasks. Cell cultures were maintained at 37°C with 5 % CO_2 and split 1:4 at a seeding density of 10^6 cells. For differentiation, THP-1 cells were seeded in 6-well plates at a density of $3x10^5$ cells and treated with 2.5 ng/ml phorbol-12-myristate-13-acetate (PMA) for 48 hrs. Prior to lipopolysaccharide (LPS) activation and treatment, cells were allowed to rest in culture media for 24 hrs. Human peripheral blood mononuclear cells (PBMCs) were isolated using Ficoll-Paque Plus (GE healthcare) density gradient centrifugation from donated blood of healthy volunteers. After centrifugation, the PBMC layers were isolated and washed with PBS to remove erythrocytes and granulocytes. PBMCs purification was performed using anti-human CD14 magnetic beads (Miltenyi Biotec) according to the manufacturer's instructions. Monocytes were maintained in RPMI 1640 (Gibco, Thermo Scientific) with 10 % FCS (Gibco, Thermo Scientific), 2 mM glutamine (Gibco, Thermo Scientific), 100 U/mL penicillin and 100 µg/mL streptomycin (Gibco, Thermo Scientific). For macrophage differentiation and maturation, human monocytes were plated onto tissue culture-treated 24-well plates at a density of 3×10^5 cells/well. The medium was supplemented with 100 ng/mL recombinant human M-CSF using CellXVivo^{TM} kit (R&D Systems) and differentiated for 5–7 days prior to use.

Cells were incubated with 1 µg/ml LPS (Invitrogen, Sweden) for 6 hrs prior to a 12 hrs treatment with 1 µM simvastatin (Bio-techne, UK), 10 µM hydralazine (Sigma-Aldrich) and/or a combination of both. The concentrations were chosen based on the dosing regimen administered in the *in vivo* studies. After incubation, cells were detached using cold PBS containing EDTA (5 mM) and either stained for flow cytometry or centrifuged and processed for RNA and protein isolation using the Trizol method.

Western Blotting, qPCR, ELISA and histological experiments: Standard biochemical procedures were utilized for experiments involving reverse transcription polymerase chain reaction, quantitative PCR, Western blotting and histological experiments. Methodological details are provided in the data supplement.

Statistical analysis: All data are expressed as mean ± SEM, where N is the number of animals or independent cell experiments. For comparisons of young and aged WT and ApoE$^{-/-}$ mice, two-way ANOVA with Sidak post hoc testing was used to assess the effects of genotype and age. For comparison of multiple independent groups, the parametric one-way ANOVA test was used, followed by Tukey's post hoc testing with exact P value computation. In case of non-normally distributed data (tested with Shapiro-Wilk test), the non-parametric Kruskal Wallis test with Dunn's post hoc testing and exact P value computation was used for multiple comparisons. For comparison of two groups a two-tailed unpaired t-test was utilized. Differences were considered significant at error probabilities of $P \leq 0.05$.

Results

1. Chronic hypercholesterolemia contributes to the development of memory impairment: To investigate whether chronic exposure to higher-than-normal plasma cholesterol levels affects important brain functions (i.e. cognition) during ageing, we tested memory function in normocholesterolemic WT and hypercholesterolemia ApoE$^{-/-}$ mice at different ages (4 and 12 months; Fig.1A). In accordance with the increased cardiovascular burden in ApoE$^{-/-}$ compared to WT mice (i.e. significantly higher plasma cholesterol levels at 4 and 12 months of age, higher systolic BP at 12 months of age; **Table 1**), long-term (hippocampus-dependent) memory function deteriorated with age in ApoE$^{-/-}$ mice, resulting in significantly lower recognition indices (RI) compared to age-matched WT controls (RI≤0.5; Fig.2A). Although neither aged WT nor aged ApoE$^{-/-}$ mice presented with signs of short-term (rhino-cortical) memory impairment when compared to their young controls (Table S1), spatial short-term memory was compromised in aged ApoE$^{-/-}$ mice as evident by a lower RI obtained in an object placement test (RI≤0.5; Fig.2B). When testing for age-related changes in pre- and post-synaptic proteins in whole brain lysates of ApoE$^{-/-}$ mice, no differences in expression of synaptosomal associated protein (SNAP-25) or postsynaptic density protein 95 (PSD-95) were observed (Fig.2C). In accordance with previous studies,[25] however, ageing affected hippocampal but not cortical PSD-95 mRNA expression in ApoE$^{-/-}$ mice (Fig.2D). Taken together, these data imply brain region-specific negative effects of early and chronic hypercholesterolemia on memory function later in life.

2. Pro-inflammatory monocytes infiltrate the brain of aged ApoE$^{-/-}$ but not WT mice: In chronically hypercholesterolemic ApoE$^{-/-}$ mice, ageing associated to apparent immune system activation as evident by a higher number of circulating Ly6Chi monocytes (Fig.3A) and elevated plasma levels of interleukin (IL)12/23 (Fig.3B). The latter often secreted by activated monocytes/macrophages promote T helper (Th) 1 and Th17 priming of T-cells,[34] which secrete IL17 amongst other cytokines and are considered main contributors to tissue inflammation.[35] Elevated IL17 plasma levels in aged ApoE$^{-/-}$ mice (Fig.3C) led us to test immune cell infiltration into brain tissue. FACS analyses revealed an increase of Ly6Chi pro-inflammatory monocytes (Fig.3D) and an overall higher percentage of CD3+ cells in brain tissue of aged vs. young ApoE$^{-/-}$ mice (Fig.3E). In line with previous publications,[36] transcripts of key chemokines that regulate migration and infiltration of monocytes and macrophages, such as monocyte chemoattractant protein-1 (MCP-1) and chemokine ligand-2 (CXCL2) were drastically elevated in brain tissue of the aged cohort compared to young control mice (**Table 2**). Moreover, an mRNA expression pattern typical of a pro-inflammatory phenotype was predominant in brain tissue of aged ApoE$^{-/-}$ mice (**Table 2**: IL6 (2.6-fold), iNOS (11.9-fold), TNF-α (3.2-fold), and IL12 (5.6-fold)) compared to young ApoE$^{-/-}$ controls. The degree of cytokine expression was brain region-dependent as evidenced by a markedly higher hippocampal than cortical IL12 expression in aged ApoE$^{-/-}$ mice compared to young controls (**Table 2**: 9.25-fold in hippocampus tissue vs. 4.91-fold in cortex tissue). IL23 also showed such region-specific expression patterns (**Table 2**: 4.76-fold in hippocampus tissue vs. 2.0-fold in cortex tissue). Besides, Arginase-1 (Arg-1) as commonly used marker for an alternatively activated macrophage phenotype presented with region-specific expression patterns: while cortical Arg-1 mRNA levels remained unaffected by age, the basally higher hippocampal Arg-1 expression significantly reduced with age (**Table 2**). Together, these data point to an apparent age-related inflammation in the hippocampus and may explain the more pronounced hippocampal-dependent memory impairment in aged ApoE$^{-/-}$ mice.

Although WT mice presented with an age-related increase of plasma cholesterol, BP (**Table 1**) and circulating Ly6Chi pro-inflammatory monocytes (Fig.3F), the percentage of Ly6Chi monocytes remained unaltered in the brain of aged WT mice (Fig.3G). Notably compared to WT mice, ApoE$^{-/-}$ mice already showed a significantly higher proportion of circulating Ly6Chi cells at young age (Fig.3F), suggesting a persistent pro-inflammatory state in chronically hypercholesterolemic ApoE$^{-/-}$ mice, which may promote immune infiltration into the brain with implications for memory function. Correspondingly, the proportion of brain Ly6Chi monocytes was higher in ApoE$^{-/-}$ mice compared to age-matched WT mice (Fig.3G). Furthermore, brain tissue of aged ApoE$^{-/-}$ mice presented with significantly higher transcripts levels of chemokines MCP-1 and CXCL2 compared to aged-matched WT controls (**Table S2**). Taken together, these data suggest a key role for Ly6Chi monocyte activation and brain infiltration during chronic hypercholesterolemia where also memory deficits were observed.

3. Cholesterol- and/or BP-lowering therapy attenuates neuro-inflammation and memory deficits in aged ApoE$^{-/-}$ mice. As chronically hypercholesterolemic ApoE$^{-/-}$ mice at 12 months of age presented with marginally elevated BP compared to 4 months old ApoE$^{-/-}$ mice, we subjected aged ApoE$^{-/-}$ mice (i.e. 12 months of age) to lipid-lowering or BP-lowering therapy for 8 consecutive weeks, using the statin simvastatin (5 mg/kg/d), the smooth muscle relaxant hydralazine (0.5 mg/kg/d). Because we did not anticipate statin-mediated effects on BP, we also administered a combination of the two drugs to a group of animals (Fig.1B). The doses administered correspond to therapeutic doses used in the clinic (10 mg/kg/d and 20 mg/kg/d, respectively). All treatment strategies proved similarly effective in lowering the age-related elevated systolic BP: longitudinal BP measurements revealed markedly lower BP values in mice post treatment compared to the recorded pre-treatment values (Fig.S1). As expected, simvastatin treatment revealed significant cholesterol-lowering effects (Table S3). In line with other investigations,[37, 38] simvastatin treatment markedly reduced the age-related elevated heart-to-body weight ratio in our model without significantly affecting heart rate (Table S3). Interestingly, simvastatin's effects on heart hypertrophy and cholesterol were diminished in the presence of hydralazine (Table S3). Simvastatin revealed considerable anti-inflammatory capacity as evident by a reduction of circulating plasma IL12/23 levels (Fig.4A) and IL17 levels *in vivo* (Fig.4B). In the brain, simvastatin-treated mice revealed lower transcript levels of pro-inflammatory cytokines and chemokines, including IL6 and IL12, MCP-1 and CXCL2 (**Table 3**). Notably, hydralazine attenuated simvastatin's effects for some of the cytokines when administered in combination (**Table 3**). Treatment affected brain regions to different degrees as supported by statistically significant differences in hippocampal but not cortical IL12 expression between simvastatin- and hydralazine-treated groups (**Table 3**). Interestingly, IL23 revealed a different expression profile with significantly lower cortical IL23 expression in simvastatin-containing treatment groups while hippocampal IL23 expression only significantly changed when mice received simvastatin alone (**Table 3**). Moreover, the age-related increase of CD68 (monocyte/macrophage activation marker) was significantly lower in groups treated with simvastatin (Fig.4C). Since a majority of CD68+ cells were positive for ionized calcium-binding adapter molecule-1 (Iba-1; common microglia/macrophage marker) we assessed how age and treatment affected the number of total and CD68+ brain macrophages, and investigated their morphology by counting the numbers of ramified (= resting), intermediate and round (= activated) Iba-1+ cells. Ageing associated to increased numbers of CD68+ Iba1+ cells in two hippocampus regions (i.e. CA1 and DG) but not in the cortex of ApoE$^{-/-}$ mice (Fig.4D/E & Fig.S2), indicative of region-specific augmentation of macrophage activation. Both hydralazine- and simvastatin-treated mice presented with lower numbers of CD68+ Iba1+ cells in the CA1 region of the hippocampus (Fig.4D); yet, only simvastatin revealed similar responses in the DG (Fig.4E). Neither drug affected CD68+ Iba-1+ cell counts in the cortex (Fig.S2). The total number of Iba-1+ cells significantly increased with age in the CA1 region of the hippocampus (Fig.4F) but not in DG or cortex (Fig.S3A/3B), suggesting region-specific proliferation of resident macrophages or accumulation of monocyte-derived macrophages. Yet, significant age-related changes in Iba-1+ cell morphology were only observed in the hippocampal DG region as evident by reduced proportion of ramified and increased amount of intermediate microglia (73.04 ± 4.53 vs. 90.97 ± 1.65, P=0.0468 and 25.61 ± 4.69 vs. 9.03 ± 1.64, P=0.0500; Table S4), adding to the notion that age elicits brain region-specific responses in chronically hypercholesterolemic mice.

Treatment differently affected overall Iba-1+ cell number and morphology. While hydralazine treatment showed no apparent effects in any of the investigated brain regions (Table S4; Fig.4F; Fig.S3A/B), mice treated with simvastatin presented with a markedly lower overall count of Iba-1+ cells (Fig.4F) and significantly reduced percentage of ramified and increased quantity of intermediate Iba-1+ cells compared to aged ApoE$^{-/-}$ mice in the hippocampal CA1 region (72.69 ± 3.55 vs. 95.08 ± 1.25, P=0.0777 and 24.88 ± 3.26 vs. 4.92 ± 1.25, P=0.0060; Table S4) and in the cortex (66.39 ± 4.30 vs. 93.10 ± 0.59, P=0.0001 and 30.51 ± 4.18 vs. 6.90 ± 0.59, P=0.0003; Table S4). Interestingly, simvastatin-treated mice presented with overall lower numbers of Iba-1+ cells compared to young ApoE$^{-/-}$ in both hippocampal DG and cortex (Fig.S3A/B) and marked changes in Iba-1+ cell morphology in all brain regions (Table S4). Similarly, combination treatment significantly reduced the number of ramified cells compared to young ApoE$^{-/-}$ mice in all brain regions investigated but markedly increased the proportion of activated cells compared to aged ApoE$^{-/-}$ in the hippocampal brain region without affecting overall Iba-1+ cell counts (Table S4; Fig.4F; Fig.S3A/B). Macrophages are highly plastic and adopt a variety of phenotypes on the scale between classically activated and alternatively activated phenotypes in response to various stimuli.[39] Simvastatin treatment attenuated the expression of several markers characteristic for classical activation (i.e. TNF-α, IL6, iNOS; **Table 3**) and significantly mitigated CD86 expression (Fig.3G) that has been shown to involve in pro-inflammatory phenotype-mediated retinal degeneration and Alzheimer´s disease (AD).[40, 41] Of markers typical of alternatively activated macrophages only Arg-1 was detected in cortical and hippocampal brain tissue in our model. Arg-1 mRNA expression significantly reduced with age in ApoE$^{-/-}$ mice, but aged mice treated with simvastatin presented with higher hippocampal Arg-1 mRNA expression (**Table 3**). Together, these data are suggestive of brain region-specific macrophage activation during ageing in ApoE$^{-/-}$ mice and an alternatively activated phenotype predominance after simvastatin treatment. Lastly, the age-related accumulation of CD3 was diminished in all treatment groups (Fig.4H).

In an open field test, only simvastatin treatment significantly improved age-related impaired mobility in ApoE$^{-/-}$ mice (Fig.5A). Combination treatment with hydralazine revealed no apparent effects on mobility; yet, statistical analysis disclosed no difference to young control. Likewise, hippocampal-dependent memory function (Fig.5B) and spatial short-term memory function (Fig.5C) significantly improved in all treatment groups containing simvastatin. BDNF, an important regulator of white matter integrity, hippocampal long-term potentiation and consequently, learning and memory,[42] was negatively affected by age in ApoE$^{-/-}$ mice, and only simvastatin treatment mitigated the age-related reduction of hippocampal BDNF expression (Fig.5D). Similarly, immune staining of hippocampal BDNF and the neuronal marker NeuN revealed evident differences between young and aged mice (Table S5, representative images shown in Fig.5E*ii-vi*). When normalized to the number of NeuN+ cells, BDNF expression was significantly lower in aged brains compared to young ApoE$^{-/-}$ mice (1.377 ± 0.054 vs. 0.781 ± 0.027; P=0.0286), and only significantly higher after treatment with simvastatin alone (Fig.5E). NeuN immunostaining, however, was significantly higher in all treatment groups that received simvastatin compared to untreated aged ApoE$^{-/-}$ mice (797.5 ± 35.8 ± 51.4 vs. 558.5 ± 55.8; P=0.050 after simvastatin treatment and 807.3 ± 50.1 vs. 558.5 ± 55.8; P=0.042 after combination treatment; Table S5). Similar to the hippocampus, immune staining for BDNF in the cortex revealed significant differences between young and aged ApoE$^{-/-}$ mice, but all treatment regimens presented with high BDNF protein expression in this brain region (Table S5). Most notably, however, NeuN immune staining only significantly differed in hippocampus but not cortex where neither age nor treatment affected NeuN expression (698.8 ± 55.9 vs. 768.0 ± 55.5; P=0.911 for aged vs. young ApoE$^{-/-}$ mice; Table S5), further supporting a prominent hippocampus-dependent memory impairment in aged chronically hypercholesterolemia ApoE$^{-/-}$ mice.

4. Simvastatin and hydralazine exert cell-specific effects. The observed differences of simvastatin and hydralazine responses *in vivo*, led us to evaluate their effects *in vitro*. Utilizing human monocytic cells (THP-1) and freshly isolated human monocytes allowed us to assess drug effects not only in monocytes but also in monocyte-derived macrophages. In both cell systems, hydralazine significantly induced cell activation (i.e. increased CD69 expression) that affected monocytes with a higher magnitude than macrophages (1.8-fold vs.

1.3-fold and 2.0-fold vs. 1.2-fold in THP-1 cells and primary cells, respectively; Fig.6A*i-iv*). Simvastatin presented with no appreciable effects on CD69 expression (Fig.6B*i-ii*). Similar to CD69, hydralazine but not simvastatin increased monocyte and macrophage CD3 expression (Fig.S4), which has been shown to involve in the delivery of pro-inflammatory cytokines (i.e. TNF-α) by macrophages.[43] Pro-inflammatory cytokine profiling in THP-1 cells revealed that LPS-induced augmentation of TNF-α protein expression only reversed with simvastatin but not hydralazine (Fig.6C). Interestingly, LPS-induced increases of intracellular IL6 protein abundance was not changed by simvastatin treatment but exacerbated in the presence of hydralazine (Fig.6D*i-v*). Hydralazine alone (without LPS pre-stimulation) disclosed similar pro-inflammatory effects (Fig.6E*i-iv*). Different from monocytic cells, LPS-induced IL6 expression was similarly reduced in the presence of simvastatin or hydralazine in PMA-differentiated THP-1 cells (Fig.S5), further indicating cell type-specific drug responses. In support of this, LPS-induced elevation of TNF-α and IL6 secretion in murine bone-marrow-derived macrophages (BMDMs) reduced with both simvastatin and hydralazine treatment (Fig.6F&G). Moreover, we detected lower surface expression of activation markers (i.e. CD86, CD80) in BMDMs of all treatment groups (Fig.S6). Additional flow cytometric analyses of monocytic or PMA-differentiated THP-1 cells revealed a strong pro-inflammatory effect of hydralazine in monocytic cells (i.e. augmentation of LPS-associated CD14+ CD16+ surface expression; 2.5-fold; Fig.S7A/B) compared to PMA-differentiated THP-1 cells. Interestingly, none of the drugs showed effects on T-cell activation (Fig.S8). Together, these data suggest cell type-specific drug effects that may benefit simvastatin as it exerted anti-inflammatory effects in both monocytic cells and monocyte-derived macrophages. Hydralazine on the other hand, induced pro-inflammatory signatures especially in monocytic cells with potential implications for conditions characterized by elevated monocyte counts like chronic hypercholesterolemia, which may explain some of the effects we observe *in vivo*.

Discussion

In this present study, we provide compelling evidence that chronic hypercholesterolemia majorly contributes to the development of memory impairment, involving pro-inflammatory processes. Our data imply that mainly the modulation of monocyte activation and thus, the stimulation of related pro-inflammatory signaling mediators critically determine the effectiveness of CVD therapeutics for improving impaired memory function associated to chronic hypercholesterolemia. Although our results indicate a link between age, hypercholesterolemia and marginally elevated BP, our data suggest that cholesterol-lowering rather than BP-lowering therapy attenuates memory impairment associated to chronic hypercholesterolemia in aged ApoE$^{-/-}$ mice.

The herein established link between chronically elevated plasma cholesterol and the development of memory impairment in aged mice is based on findings, showing that only early exposure to elevated plasma cholesterol (i.e. as evident in ApoE$^{-/-}$ mice already at 4 months of age), indicative of chronic hypercholesterolemia results in reduced long-term and spatial memory function at an older age (i.e. 12 months of age). This conclusion aligns with data obtained in epidemiological studies supporting a correlation between early- or mid-life cholesterol levels to dementia in later life.[44, 45] Similar to our findings obtained in aged WT mice, no association between cognitive decline and hypercholesterolemia was found in studies examining cholesterol levels in cohorts of older patients.[46, 47] Interestingly, it has been shown that female ApoE$^{-/-}$ mice display greater cognitive impairment than male ApoE$^{-/-}$ mice.[26, 48] The fact that female ApoE$^{-/-}$mice develop more severe atherosclerosis and vascular impairment earlier[49] supports the hypothesis that atherosclerosis contributes to cognitive dysfunction in this model. This is further signified by findings showing an absence of cognitive deficits in female brain-specific ApoE$^{-/-}$ mice that are characterized by absence of systemic hypercholesterolemia.[26] It would therefore be of interest to further investigate sex-specific effects on systemic and neuro-inflammation in the context of hypercholesterolemia. Although hypercholesterolemia was generally accompanied by higher-than-normal BP in aged ApoE$^{-/-}$ mice, cholesterol-lowering rather than BP-lowering therapy significantly improved the impaired spatial memory of aged ApoE$^{-/-}$ mice. This further positions early life exposure to high cholesterol levels as major contributor to cognitive dysfunction in addition to potential BP-mediated structural and functional alterations in the brain.[3] It needs to be noted that unlike statins for dyslipidemia treatment,

hydralazine is not the first line medication for treating elevated BP. Nonetheless, hydralazine appears as first choice of BP-lowering therapy in numerous experimental studies where it has mostly been used preventatively to investigate the link between hypertension and inflammation or cognitive function,[3, 50, 51] and is often used in the clinic to treat preeclampsia. Besides its vasorelaxant properties, it is thought to exert effects on the immune system. A few reports have assigned hydralazine with anti-inflammatory properties, resulting from reduced ICAM- and P-selectin- mediated T-cell transmigration[28] and induced T-cell apoptosis.[52] However, hydralazine-induced increases of cellular CD3-zeta chain content in T-cells are discussed to facilitate excessive drug-induced auto-immunity.[53] The pronounced enhancement of monocytic cell activation we observed in the presence of hydralazine might be resultant from reactive metabolites deriving from hydralazine oxidation[54] or from hydralazine-mediated inhibition of DNA methyltransferase,[55] which are postulated as major mechanisms in drug-induced auto-immunity,[54] and might limit its potency to resolve neuro-inflammatory processes and thus, improve memory deficits in our model. Moreover, it might limit therapeutic efficacy of other drugs when administered in combination. This effect calls for the need to test for potential interactions between BP-lowering drugs of different nature and statins for potential consequences on immune regulation and cognitive impairment. Considering current knowledge in the field that suggests prominent involvement of the renin-angiotensin system (RAS) in the development of neurodegenerative diseases which has generated an appreciation for RAS-targeted treatment efficacy in hypertension-associated brain alterations, AD mouse models and early-onset AD patients, it will be of utmost importance to further investigate the value of different classes of BP-lowering drugs in multi-morbid systems. The obvious benefits of angiotensin-converting enzyme inhibitors (ACEi) to attenuating amyloid-beta (Aβ) accumulation and glia-induced inflammation and improving cognitive function in AD mouse models[56, 57] have led to epidemiological studies that showed promising associations between the use of ACEi and cognitive function in AD patients.[58] Nonetheless, their potential to modulate inflammation is similarly controversially discussed as hydralazine's immune system effects.[59, 60] Thus, the circumstances under which BP-lowering drugs exert beneficial effects by slowing neuro-inflammation or cognitive decline remain to be determined especially, in the context of multi-morbid phenotypes.

The activation of the immune system emerged as an important driver in the aged and vulnerable brain. Experimental studies verified the significance of inflammation in CVD progression[61, 62] and showed that inflammation associated to cardiovascular risk factors or CVD negatively affects cognitive function.[20, 21, 63, 64] However, precise pro-inflammatory mechanisms contributing to accelerated cognitive decline and dementia risk require further elucidation. Recently, Faraco *et al*. uncovered the Th17 - IL17 pathway as novel gut-brain-axis key player linking high dietary salt intake to cerebrovascular alterations and cognitive impairment in mice.[64] The authors report a diet-induced expansion of Th17 cells in the gut that contributes to increases in circulating IL17, which in turn, negatively affects endothelial nitric oxide signaling of the cerebral vasculature with serious consequence for brain perfusion and cognitive performance. Interestingly, these effects occur in absence of a hypertensive phenotype. In our study, we observe elevated IL17 plasma levels in cognitively impaired aged ApoE$^{-/-}$ mice with elevated cholesterol and BP levels, which further signifies the link between circulating IL17 levels and memory performance as simvastatin-induced lowering of plasma cholesterol, BP and IL17 levels improved memory function. In a different study, high-fat diet elevated plasma IL6 levels in WT and ApoE$^{-/-}$ mice, however, no difference in brain IL6 was observed.[65] Another experimental study by Dinh *et al.* convincingly associates high fat diet-induced hypercholesterolemia in aged ApoE$^{-/-}$ mice not only to elevated plasma levels of IL6, TNF-α, and IFN-γ but also higher transcript levels of pro-inflammatory chemokine MCP-1 in brain tissue of these mice.[36] In our study, we witness a similar increase of such key chemokines responsible for regulating migration and infiltration of monocytes in brain tissue of standard chow-fed aged ApoE$^{-/-}$ but not WT mice. Consequently, the accumulation of pro-inflammatory Ly6Chi monocytes in the brain of chronically hypercholesterolemic aged ApoE$^{-/-}$ mice was absent in age-matched WT mice where plasma cholesterol levels only increase later in life. Thus, our findings position pro-inflammatory monocytes as important contributors to neuro-inflammation emanating from chronic hypercholesterolemia. The concept of hypercholesterolemia-associated neuro-inflammation was recently investigated in an elegant study that

provided first insight into choroid plexus inflammation and complement activation in aged hypercholesterolemic ApoE$^{-/-}$ mice. Here, choroid plexus lipid accumulation induced leukocyte infiltration that extended to the adjacent brain parenchyma, demonstrating that lipid-triggered complement cascade activation promotes leukocyte infiltration into the choroid plexus.[27] The authors conclude that ApoE acts as checkpoint inhibitor for the complement cascade with implications for immune system activation, cognitive decline in late onset AD and atherosclerotic plaque formation.[27] Together with the finding that brain-specific ApoE deficiency protects from cognitive decline in the absence of hypercholesterolemia,[26] this further signifies the importance of chronic hypercholesterolemia in neuro-inflammatory and -degenerative processes observed in our model. The herein characterized brain region-specific neuro-inflammation (i.e. brain macrophage proliferation and activation, cytokine expression) together with distinct brain region-specific changes after cholesterol-lowering therapy, however, also suggest additional simvastatin-mediated mechanisms independent of cholesterol-lowering.

Our herein presented experimental strategy demonstrates that simvastatin therapy proves effective in reducing neuro-inflammation associated to chronic hypercholesterolemia in aged ApoE$^{-/-}$ mice. In particular, its beneficial hippocampal-specific effects on Iba-1+ cell number and morphology, CD86 and Arg-1 expression in our model point to additional therapeutic mechanisms independent of cholesterol-lowering. Simvastatin's anti-inflammatory character might be resultant from its potency to regulating proliferation and activation of monocytes and macrophages,[22, 29] and to modulating myeloid cell phenotype[66] and secretory function.[67, 68] Monocyte-derived immature dendritic cells and type 1 macrophages respond to simvastatin-induced down-regulation of MCP-1,[69] which may impact their chemotactic activity and thus, reduce their recruitment to sites of tissue injury. The herein presented *in vitro* findings describe simvastatin's direct therapeutic effect on monocyte and macrophage activation and extent previous reports that showed an effective reduction of cytokine secretion in PMA-differentiated THP-1 cells pre-treated with simvastatin.[67] In its role as modulator for IL secretion from monocytes and macrophages, simvastatin was shown to indirectly inhibit IL17 secretion from CD4+ T-cells.[70] Moreover, simvastatin has been shown to directly inhibit the expression of a transcription factor responsible for controlling IL17 production in CD4+ T-cells.[70] These findings are in line with our herein presented data showing a reduction of IL17 plasma levels *in vivo* only after simvastatin treatment. However, it remains to be determined whether the simvastatin effects in our model are mediated through direct modulation of Th17 responses, indirectly through modulation of myeloid cell activation or primarily through its lipid-lowering capacity. Because simvastatin has also been associated to Th2 immune response and neuronal recovery[71, 72] we cannot exclude a potential therapeutic effect on T-cells in our model. Nonetheless, our results point to therapeutic effects through monocyte modulation, which aligns with studies conducted in patients at high risk for vascular events where a simvastatin-induced down-regulation of the angiotensin II type 1 receptor on monocytes but not T-cells significantly affected angiotensin II activity and thus, contributes to its anti-inflammatory profile and therapeutic effects in CVD.[73] Moreover, in patients with hypercholesterolemia, simvastatin was shown to reduce monocyte secretory function.[68, 74] Most interestingly in respect to neurodegeneration is a study reporting a lowering of the CD14+CD16+ "intermediate" monocyte subset in purified monocytes isolated from peripheral blood of HIV patients in response to an *ex vivo* treatment with simvastatin, as this particular subset of monocytes is closely linked to HIV-associated neurocognitive disorders.[66]

Despite the availability of case reports discussing adverse effects of statins on cognitive function,[15, 16] our study describes favorable outcomes for memory function in aged ApoE$^{-/-}$ mice after statin therapy. Although lipophilic statins, such as simvastatin are thought to cross the blood–brain barrier, leading to a reduction of cholesterol availability and thereby, disturbing the integrity of the neuronal and glial cell membrane,[75] simvastatin treatment had no negative effects on hippocampal neurons, and significantly increased hippocampal and cortical BDNF expression in our model. However, it has been reported that hydrophilic statins exert negative effects on learning and recognition memory, which is reversed upon discontinuation.[76] In contrast to the published case reports showing statin-induced memory loss,[15, 16] two large randomized control trials on

simvastatin[77] and pravastatin[78] did not identify a relationship between statin use and cognitive decline. Most beneficial effects of simvastatin in the brain are thought to root from the promotion of hippocampal neurogenesis, the inhibition of mesangial cell apoptosis,[79, 80] the enhancement of neurotrophic factors, and the restriction of inflammation.[81] In light of this, simvastatin treatment markedly increased hippocampal expression of BDNF, which has been linked to improved functional recovery after stroke and the amelioration of depressive-like behavior,[13, 14] and may underlie the improvements in hippocampal-dependent memory function we observe in our model. Besides, preventative simvastatin treatment resulted in lower Aβ 40/42 levels in cerebrospinal fluid of AD mice, attenuated neuronal apoptosis and improved cognitive competence of the hippocampal network,[82] suggesting that statin treatment may prevent the age-related, progressive neuropathy characteristic for 3xTg-AD mice. Together with findings showing that high-fat diet increases Aβ levels in the brain of ApoE$^{-/-}$ mice[83] and simvastatin's capacity to reduce Aβ accumulation in primary neurons and in guinea pig brain,[84] further investigation of Aβ accumulation in respect to neuro-inflammation and its modifiability by cholesterol-lowering or anti-inflammatory therapies would certainly elevate the impact of statin therapy beyond the field of CVD and associated target organ damage.

Taken together, our study convincingly links chronic hypercholesterolemia (i.e. elevated total plasma cholesterol levels already apparent at 4 months of age in ApoE$^{-/-}$ mice) to myeloid cell activation, neuro-inflammation and memory impairment, supporting the notion that early rather than late-life exposure to cardiovascular risk factors promotes the development of cognitive dysfunction. Cholesterol-lowering therapy provides effectiveness to improving memory function potentially by reducing monocyte-driven inflammatory events and hence, emerges as safe therapeutic strategy to control CVD-induced memory impairment and represents another benefit of statins in patients with hypercholesterolemia.

<u>Study limitations and outlook:</u> Controversies regarding BP phenotype in ApoE$^{-/-}$ mice persist, however, it is difficult to draw conclusions from the current literature as studies differ in duration, diet and animal age. Dinh and colleagues reported a lack of BP elevation in aged ApoE$^{-/-}$ mice subjected to high-fat diet compared to WT mice on conventional diet.[36] A similar high-fat diet increased BP already after 12 weeks in another study.[85] In contrast to the herein presented results, an earlier study suggested no differences in BP between aged ApoE$^{-/-}$ and WT mice on normal chow diet (140 ± 7.6 mmHg in ApoE$^{-/-}$ mice and 136 ± 7.4 mmHg in WT mice).[86] The study, however, did not assess BP differences between young and aged ApoE$^{-/-}$ mice. Considering the current knowledge in the field, it remains to be further investigated whether or not changes in systemic BP contribute to the inflammatory and the brain phenotype described in this model. Furthermore, neither memory impairment nor neuro-inflammation in our study were assessed longitudinally. However, our data convincingly show apparent memory deficits and obvious signs of neuro-inflammation and -degeneration in ApoE$^{-/-}$ mice at the age of 12 months, which goes in line with findings of previously published studies.[26, 48] It is therefore likely that the applied treatment regimens not only attenuate but also reverse brain degeneration in aged ApoE$^{-/-}$ mice. In order to decipher cell type-specific treatment effects on circulating immune cells, systemic assessment of different immune-related tissue compartments would be necessary. Moreover, understanding the mechanism of action by which simvastatin or other CVD therapeutics influence neuro-inflammatory events and affect monocyte and macrophage polarization *in vivo* will require further investigation using more advanced single-cell techniques, which have recently provided important insight into the plasticity of these cell types and the existence of a wide stimuli-driven network of myeloid cell behavior[87, 88] that may drastically impact neurological performance. In line with that, it would be of interest how cholesterol- and BP-lowering therapies affect atherosclerosis progression (i.e. lesion size and plaque stability) in this model and to what extent this affects memory functions. Although statins are thought to cause regression of atherosclerosis in humans, it has been shown that the amount of lesion regression is small compared with the magnitude of the observed clinical benefit. Similarly, preclinical studies also showed beneficial statin effects on plaque stability in ApoE$^{-/-}$ mice,[89, 90] however, there seems to be an ongoing debate about their ability to actually reduce lesion size. Lastly, sex-specific differences need to be investigated as our study was solely performed in male mice. Especially since previous studies convincingly showed an increased susceptibility of female mice to the development of

cognitive impairment in response to chronic hypercholesterolemia,[26, 48] treatment responses may also differ sex-specifically.

Funding: This work was supported by the following funding sources: The Knut and Alice Wallenberg foundation [2015.0030; AM]; Swedish Research Council [VR; 2017-01243; AM]; German Research Foundation [DFG; ME 4667/2-1; AM]; Åke Wibergs Stiftelse [M19-0380; AM]; Hedlund Stiftelse [M-2019-1101; AM] and Inger Bendix Stiftelse [AM-2019-10; AM]; Stohnes Stiftelse [AM], Demensfonden [AM], and startup funds provided by the Wallenberg Centre for Molecular and Translational Medicine, University of Gothenburg, Sweden [AH].

Acknowledgement: The authors thank Dr. Anna Planas for contributing aged ApoE$^{-/-}$ mice and allowing us to use her behavioral platform, Francisca Ruiz for help with the treatment of the ApoE$^{-/-}$ mice and the support with Elisa experiments, Dr. Harry Björkbacka for providing aged ApoE$^{-/-}$ mice and access to his flow cytometer, and Yun Zhang for help with running some of the flow cytometry.

Conflict of Interest: None declared.

Data Availability: The data underlying this article are available in the article and in its online supplementary material.

References

1. Wimo A, Jonsson L, Gustavsson A, McDaid D, Ersek K, Georges J, Gulacsi L, Karpati K, Kenigsberg P and Valtonen H. The economic impact of dementia in Europe in 2008-cost estimates from the Eurocode project. *International journal of geriatric psychiatry*. 2011;26:825-32.
2. Meissner A. Hypertension and the Brain: A Risk Factor for More Than Heart Disease. *Cerebrovascular diseases*. 2016;42:255-62.
3. Meissner A, Minnerup J, Soria G and Planas AM. Structural and functional brain alterations in a murine model of Angiotensin II-induced hypertension. *Journal of neurochemistry*. 2016.
4. Gasecki D, Kwarciany M, Nyka W and Narkiewicz K. Hypertension, brain damage and cognitive decline. *Current hypertension reports*. 2013;15:547-58.
5. Moreira EL, de Oliveira J, Nunes JC, Santos DB, Nunes FC, Vieira DS, Ribeiro-do-Valle RM, Pamplona FA, de Bem AF, Farina M, Walz R and Prediger RD. Age-related cognitive decline in hypercholesterolemic LDL receptor knockout mice (LDLr-/-): evidence of antioxidant imbalance and increased acetylcholinesterase activity in the prefrontal cortex. *J Alzheimers Dis*. 2012;32:495-511.
6. van Vliet P. Cholesterol and late-life cognitive decline. *J Alzheimers Dis*. 2012;30 Suppl 2:S147-62.
7. Hajjar I, Hart M, Chen YL, Mack W, Milberg W, Chui H and Lipsitz L. Effect of antihypertensive therapy on cognitive function in early executive cognitive impairment: a double-blind randomized clinical trial. *Archives of internal medicine*. 2012;172:442-4.
8. Rigaud AS, Olde-Rikkert MG, Hanon O, Seux ML and Forette F. Antihypertensive drugs and cognitive function. *Current hypertension reports*. 2002;4:211-5.
9. Peters R, Beckett N, Forette F, Tuomilehto J, Clarke R, Ritchie C, Waldman A, Walton I, Poulter R, Ma S, Comsa M, Burch L, Fletcher A, Bulpitt C and investigators H. Incident dementia and blood pressure lowering in the Hypertension in the Very Elderly Trial cognitive function assessment (HYVET-COG): a double-blind, placebo controlled trial. *The Lancet Neurology*. 2008;7:683-9.
10. Chang-Quan H, Hui W, Chao-Min W, Zheng-Rong W, Jun-Wen G, Yong-Hong L, Yan-You L and Qing-Xiu L. The association of antihypertensive medication use with risk of cognitive decline and dementia: a meta-analysis of longitudinal studies. *International journal of clinical practice*. 2011;65:1295-305.
11. Jick H, Zornberg GL, Jick SS, Seshadri S and Drachman DA. Statins and the risk of dementia. *Lancet*. 2000;356:1627-31.
12. Rockwood K, Kirkland S, Hogan DB, MacKnight C, Merry H, Verreault R, Wolfson C and McDowell I. Use of lipid-lowering agents, indication bias, and the risk of dementia in community-dwelling elderly people. *Archives of neurology*. 2002;59:223-7.
13. Ludka FK, Cunha MP, Dal-Cim T, Binder LB, Constantino LC, Massari CM, Martins WC, Rodrigues AL and Tasca CI. Atorvastatin Protects from Abeta1-40-Induced Cell Damage and Depressive-Like Behavior via ProBDNF Cleavage. *Mol Neurobiol*. 2016.
14. Zhang J, Mu X, Breker DA, Li Y, Gao Z and Huang Y. Atorvastatin treatment is associated with increased BDNF level and improved functional recovery after atherothrombotic stroke. *Int J Neurosci*. 2017;127:92-97.
15. Suraweera C, de Silva V and Hanwella R. Simvastatin-induced cognitive dysfunction: two case reports. *Journal of medical case reports*. 2016;10:83.
16. Wagstaff LR, Mitton MW, Arvik BM and Doraiswamy PM. Statin-associated memory loss: analysis of 60 case reports and review of the literature. *Pharmacotherapy*. 2003;23:871-80.
17. Pietschmann P, Gollob E, Brosch S, Hahn P, Kudlacek S, Willheim M, Woloszczuk W, Peterlik M and Tragl KH. The effect of age and gender on cytokine production by human peripheral blood mononuclear cells and markers of bone metabolism. *Experimental gerontology*. 2003;38:1119-27.
18. Tan ZS and Seshadri S. Inflammation in the Alzheimer's disease cascade: culprit or innocent bystander? *Alzheimer's research & therapy*. 2010;2:6.
19. McRae A, Dahlstrom A, Polinsky R and Ling EA. Cerebrospinal fluid microglial antibodies: potential diagnostic markers for immune mechanisms in Alzheimer's disease. *Behavioural brain research*. 1993;57:225-34.
20. Meissner A, Visanji NP, Momen MA, Feng R, Francis BM, Bolz SS and Hazrati LN. Tumor Necrosis Factor-alpha Underlies Loss of Cortical Dendritic Spine Density in a Mouse Model of Congestive Heart Failure. *Journal of the American Heart Association*. 2015;4.
21. Don-Doncow N, Vanherle L, Zhang Y and Meissner A. T-Cell Accumulation in the Hypertensive Brain: A Role for Sphingosine-1-Phosphate-Mediated Chemotaxis. *Int J Mol Sci*. 2019;20.

22. Alaarg A, Zheng KH, van der Valk FM, da Silva AE, Versloot M, van Ufford LC, Schulte DM, Storm G, Metselaar JM, Stroes ES and Hamers AA. Multiple pathway assessment to predict anti-atherogenic efficacy of drugs targeting macrophages in atherosclerotic plaques. *Vascular pharmacology*. 2016;82:51-9.
23. Sparrow CP, Burton CA, Hernandez M, Mundt S, Hassing H, Patel S, Rosa R, Hermanowski-Vosatka A, Wang PR, Zhang D, Peterson L, Detmers PA, Chao YS and Wright SD. Simvastatin has anti-inflammatory and antiatherosclerotic activities independent of plasma cholesterol lowering. *Arteriosclerosis, thrombosis, and vascular biology*. 2001;21:115-21.
24. Kitayama J, Faraci FM, Lentz SR and Heistad DD. Cerebral vascular dysfunction during hypercholesterolemia. *Stroke*. 2007;38:2136-41.
25. Masliah E, Mallory M, Ge N, Alford M, Veinbergs I and Roses AD. Neurodegeneration in the central nervous system of apoE-deficient mice. *Exp Neurol*. 1995;136:107-22.
26. Lane-Donovan C, Wong WM, Durakoglugil MS, Wasser CR, Jiang S, Xian X and Herz J. Genetic Restoration of Plasma ApoE Improves Cognition and Partially Restores Synaptic Defects in ApoE-Deficient Mice. *J Neurosci*. 2016;36:10141-50.
27. Yin C, Ackermann S, Ma Z, Mohanta SK, Zhang C, Li Y, Nietzsche S, Westermann M, Peng L, Hu D, Bontha SV, Srikakulapu P, Beer M, Megens RTA, Steffens S, Hildner M, Halder LD, Eckstein HH, Pelisek J, Herms J, Roeber S, Arzberger T, Borodovsky A, Habenicht L, Binder CJ, Weber C, Zipfel PF, Skerka C and Habenicht AJR. ApoE attenuates unresolvable inflammation by complex formation with activated C1q. *Nat Med*. 2019;25:496-506.
28. Rodrigues SF, de Oliveira MA, dos Santos RA, Soares AG, de Cassia Tostes R, Carvalho MH and Fortes ZB. Hydralazine reduces leukocyte migration through different mechanisms in spontaneously hypertensive and normotensive rats. *European journal of pharmacology*. 2008;589:206-14.
29. Rezaie-Majd A, Maca T, Bucek RA, Valent P, Muller MR, Husslein P, Kashanipour A, Minar E and Baghestanian M. Simvastatin reduces expression of cytokines interleukin-6, interleukin-8, and monocyte chemoattractant protein-1 in circulating monocytes from hypercholesterolemic patients. *Arteriosclerosis, thrombosis, and vascular biology*. 2002;22:1194-9.
30. Mullen L, Ferdjani J and Sacre S. Simvastatin inhibits TLR8 signaling in primary human monocytes and spontaneous TNF production from rheumatoid synovial membrane cultures. *Molecular medicine*. 2015.
31. Nair AB and Jacob S. A simple practice guide for dose conversion between animals and human. *J Basic Clin Pharm*. 2016;7:27-31.
32. Lidington D, Fares JC, Uhl FE, Dinh DD, Kroetsch JT, Sauve M, Malik FA, Matthes F, Vanherle L, Adel A, Momen A, Zhang H, Aschar-Sobbi R, Foltz WD, Wan H, Sumiyoshi M, Macdonald RL, Husain M, Backx PH, Heximer SP, Meissner A and Bolz SS. CFTR Therapeutics Normalize Cerebral Perfusion Deficits in Mouse Models of Heart Failure and Subarachnoid Hemorrhage. *JACC Basic Transl Sci*. 2019;4:940-958.
33. Baker KB and Kim JJ. Effects of stress and hippocampal NMDA receptor antagonism on recognition memory in rats. *Learning & memory*. 2002;9:58-65.
34. Aggarwal S, Ghilardi N, Xie MH, de Sauvage FJ and Gurney AL. Interleukin-23 promotes a distinct CD4 T cell activation state characterized by the production of interleukin-17. *J Biol Chem*. 2003;278:1910-4.
35. Damsker JM, Hansen AM and Caspi RR. Th1 and Th17 cells: adversaries and collaborators. *Annals of the New York Academy of Sciences*. 2010;1183:211-21.
36. Dinh QN, Chrissobolis S, Diep H, Chan CT, Ferens D, Drummond GR and Sobey CG. Advanced atherosclerosis is associated with inflammation, vascular dysfunction and oxidative stress, but not hypertension. *Pharmacological research*. 2017;116:70-76.
37. Patel R, Nagueh SF, Tsybouleva N, Abdellatif M, Lutucuta S, Kopelen HA, Quinones MA, Zoghbi WA, Entman ML, Roberts R and Marian AJ. Simvastatin induces regression of cardiac hypertrophy and fibrosis and improves cardiac function in a transgenic rabbit model of human hypertrophic cardiomyopathy. *Circulation*. 2001;104:317-24.
38. Takemoto M, Node K, Nakagami H, Liao Y, Grimm M, Takemoto Y, Kitakaze M and Liao JK. Statins as antioxidant therapy for preventing cardiac myocyte hypertrophy. *The Journal of clinical investigation*. 2001;108:1429-37.
39. Ma Y, Wang J, Wang Y and Yang GY. The biphasic function of microglia in ischemic stroke. *Prog Neurobiol*. 2017;157:247-272.
40. Zhou T, Huang Z, Sun X, Zhu X, Zhou L, Li M, Cheng B, Liu X and He C. Microglia Polarization with M1/M2 Phenotype Changes in rd1 Mouse Model of Retinal Degeneration. *Front Neuroanat*. 2017;11:77.
41. Zhang F, Zhong R, Li S, Fu Z, Cheng C, Cai H and Le W. Acute Hypoxia Induced an Imbalanced M1/M2 Activation of Microglia through NF-kappaB Signaling in Alzheimer's Disease Mice and Wild-Type Littermates. *Front Aging Neurosci*. 2017;9:282.

42. Bekinschtein P, Cammarota M, Katche C, Slipczuk L, Rossato JI, Goldin A, Izquierdo I and Medina JH. BDNF is essential to promote persistence of long-term memory storage. *Proceedings of the National Academy of Sciences of the United States of America*. 2008;105:2711-6.
43. Rodriguez-Cruz A, Vesin D, Ramon-Luing L, Zuniga J, Quesniaux VFJ, Ryffel B, Lascurain R, Garcia I and Chavez-Galan L. CD3(+) Macrophages Deliver Proinflammatory Cytokines by a CD3- and Transmembrane TNF-Dependent Pathway and Are Increased at the BCG-Infection Site. *Front Immunol*. 2019;10:2550.
44. Whitmer RA, Sidney S, Selby J, Johnston SC and Yaffe K. Midlife cardiovascular risk factors and risk of dementia in late life. *Neurology*. 2005;64:277-81.
45. Zambon D, Quintana M, Mata P, Alonso R, Benavent J, Cruz-Sanchez F, Gich J, Pocovi M, Civeira F, Capurro S, Bachman D, Sambamurti K, Nicholas J and Pappolla MA. Higher incidence of mild cognitive impairment in familial hypercholesterolemia. *Am J Med*. 2010;123:267-74.
46. Arvanitakis Z, Schneider JA, Wilson RS, Bienias JL, Kelly JF, Evans DA and Bennett DA. Statins, incident Alzheimer disease, change in cognitive function, and neuropathology. *Neurology*. 2008;70:1795-802.
47. Kivipelto M and Solomon A. Cholesterol as a risk factor for Alzheimer's disease - epidemiological evidence. *Acta Neurol Scand Suppl*. 2006;185:50-7.
48. Raber J, Wong D, Buttini M, Orth M, Bellosta S, Pitas RE, Mahley RW and Mucke L. Isoform-specific effects of human apolipoprotein E on brain function revealed in ApoE knockout mice: increased susceptibility of females. *Proceedings of the National Academy of Sciences of the United States of America*. 1998;95:10914-9.
49. Caligiuri G, Nicoletti A, Zhou X, Tornberg I and Hansson GK. Effects of sex and age on atherosclerosis and autoimmunity in apoE-deficient mice. *Atherosclerosis*. 1999;145:301-8.
50. Itani HA, McMaster WG, Jr., Saleh MA, Nazarewicz RR, Mikolajczyk TP, Kaszuba AM, Konior A, Prejbisz A, Januszewicz A, Norlander AE, Chen W, Bonami RH, Marshall AF, Poffenberger G, Weyand CM, Madhur MS, Moore DJ, Harrison DG and Guzik TJ. Activation of Human T Cells in Hypertension: Studies of Humanized Mice and Hypertensive Humans. *Hypertension*. 2016;68:123-32.
51. Iulita MF, Vallerand D, Beauvillier M, Haupert N, C AU, Gagne A, Vernoux N, Duchemin S, Boily M, Tremblay ME and Girouard H. Differential effect of angiotensin II and blood pressure on hippocampal inflammation in mice. *Journal of neuroinflammation*. 2018;15:62.
52. Ruiz-Magana MJ, Martinez-Aguilar R, Lucendo E, Campillo-Davo D, Schulze-Osthoff K and Ruiz-Ruiz C. The antihypertensive drug hydralazine activates the intrinsic pathway of apoptosis and causes DNA damage in leukemic T cells. *Oncotarget*. 2016;7:21875-86.
53. Januchowski R and Jagodzinski PP. Effect of hydralazine on CD3-zeta chain expression in Jurkat T cells. *Advances in medical sciences*. 2006;51:178-80.
54. Uetrecht J. Current trends in drug-induced autoimmunity. *Autoimmunity reviews*. 2005;4:309-14.
55. Arce C, Segura-Pacheco B, Perez-Cardenas E, Taja-Chayeb L, Candelaria M and Duennas-Gonzalez A. Hydralazine target: from blood vessels to the epigenome. *Journal of translational medicine*. 2006;4:10.
56. Asraf K, Torika N, Apte RN and Fleisher-Berkovich S. Microglial Activation Is Modulated by Captopril: in Vitro and in Vivo Studies. *Front Cell Neurosci*. 2018;12:116.
57. Dong YF, Kataoka K, Tokutomi Y, Nako H, Nakamura T, Toyama K, Sueta D, Koibuchi N, Yamamoto E, Ogawa H and Kim-Mitsuyama S. Perindopril, a centrally active angiotensin-converting enzyme inhibitor, prevents cognitive impairment in mouse models of Alzheimer's disease. *FASEB J*. 2011;25:2911-20.
58. de Oliveira FF, Bertolucci PH, Chen ES and Smith MC. Brain-penetrating angiotensin-converting enzyme inhibitors and cognitive change in patients with dementia due to Alzheimer's disease. *J Alzheimers Dis*. 2014;42 Suppl 3:S321-4.
59. Goel R, Bhat SA, Rajasekar N, Hanif K, Nath C and Shukla R. Hypertension exacerbates predisposition to neurodegeneration and memory impairment in the presence of a neuroinflammatory stimulus: Protection by angiotensin converting enzyme inhibition. *Pharmacol Biochem Behav*. 2015;133:132-45.
60. Coelho dos Santos JS, Menezes CA, Villani FN, Magalhaes LM, Scharfstein J, Gollob KJ and Dutra WO. Captopril increases the intensity of monocyte infection by Trypanosoma cruzi and induces human T helper type 17 cells. *Clin Exp Immunol*. 2010;162:528-36.
61. Berg KE, Ljungcrantz I, Andersson L, Bryngelsson C, Hedblad B, Fredrikson GN, Nilsson J and Bjorkbacka H. Elevated CD14++CD16- monocytes predict cardiovascular events. *Circulation Cardiovascular genetics*. 2012;5:122-31.
62. Meissner A, Miro F, Jimenez-Altayo F, Jurado A, Vila E and Planas AM. Sphingosine-1-phosphate signalling-a key player in the pathogenesis of Angiotensin II-induced hypertension. *Cardiovasc Res*. 2017;113:123-133.

63. Don-Doncow N, Zhang Y, Matuskova H and Meissner A. The emerging alliance of sphingosine-1-phosphate signalling and immune cells: from basic mechanisms to implications in hypertension. *Br J Pharmacol*. 2019;176:1989-2001.
64. Faraco G, Brea D, Garcia-Bonilla L, Wang G, Racchumi G, Chang H, Buendia I, Santisteban MM, Segarra SG, Koizumi K, Sugiyama Y, Murphy M, Voss H, Anrather J and Iadecola C. Dietary salt promotes neurovascular and cognitive dysfunction through a gut-initiated TH17 response. *Nat Neurosci*. 2018;21:240-249.
65. Famer D, Wahlund LO and Crisby M. Rosuvastatin reduces microglia in the brain of wild type and ApoE knockout mice on a high cholesterol diet; implications for prevention of stroke and AD. *Biochem Biophys Res Commun*. 2010;402:367-72.
66. Yadav A, Betts MR and Collman RG. Statin modulation of monocyte phenotype and function: implications for HIV-1-associated neurocognitive disorders. *Journal of neurovirology*. 2016;22:584-596.
67. McFarland AJ, Davey AK and Anoopkumar-Dukie S. Statins Reduce Lipopolysaccharide-Induced Cytokine and Inflammatory Mediator Release in an In Vitro Model of Microglial-Like Cells. *Mediators of inflammation*. 2017;2017:2582745.
68. Krysiak R and Okopien B. Monocyte-suppressing effects of simvastatin in patients with isolated hypertriglyceridemia. *European journal of internal medicine*. 2013;24:255-9.
69. Zanette DL, van Eggermond MC, Haasnoot G and van den Elsen PJ. Simvastatin reduces CCL2 expression in monocyte-derived cells by induction of a repressive CCL2 chromatin state. *Human immunology*. 2014;75:10-4.
70. Zhang X, Jin J, Peng X, Ramgolam VS and Markovic-Plese S. Simvastatin inhibits IL-17 secretion by targeting multiple IL-17-regulatory cytokines and by inhibiting the expression of IL-17 transcription factor RORC in CD4+ lymphocytes. *Journal of immunology*. 2008;180:6988-96.
71. Arora M, Chen L, Paglia M, Gallagher I, Allen JE, Vyas YM, Ray A and Ray P. Simvastatin promotes Th2-type responses through the induction of the chitinase family member Ym1 in dendritic cells. *Proceedings of the National Academy of Sciences of the United States of America*. 2006;103:7777-82.
72. Hakamada-Taguchi R, Uehara Y, Kuribayashi K, Numabe A, Saito K, Negoro H, Fujita T, Toyo-oka T and Kato T. Inhibition of hydroxymethylglutaryl-coenzyme a reductase reduces Th1 development and promotes Th2 development. *Circulation research*. 2003;93:948-56.
73. Marino F, Guasti L, Cosentino M, Rasini E, Ferrari M, Maio RC, Loraschi A, Cimpanelli MG, Schembri L, Legnaro M, Molteni E, Crespi C, Crema F, Venco A and Lecchini S. Simvastatin treatment in subjects at high cardiovascular risk modulates AT1R expression on circulating monocytes and T lymphocytes. *Journal of hypertension*. 2008;26:1147-55.
74. Krysiak R and Okopien B. Different effects of simvastatin on ex vivo monocyte cytokine release in patients with hypercholesterolemia and impaired glucose tolerance. *Journal of physiology and pharmacology : an official journal of the Polish Physiological Society*. 2010;61:725-32.
75. Miron VE, Zehntner SP, Kuhlmann T, Ludwin SK, Owens T, Kennedy TE, Bedell BJ and Antel JP. Statin therapy inhibits remyelination in the central nervous system. *Am J Pathol*. 2009;174:1880-90.
76. Stuart SA, Robertson JD, Marrion NV and Robinson ES. Chronic pravastatin but not atorvastatin treatment impairs cognitive function in two rodent models of learning and memory. *PLoS One*. 2013;8:e75467.
77. Heart Protection Study Collaborative G. Randomized trial of the effects of cholesterol-lowering with simvastatin on peripheral vascular and other major vascular outcomes in 20,536 people with peripheral arterial disease and other high-risk conditions. *J Vasc Surg*. 2007;45:645-654; discussion 653-4.
78. Shepherd J, Blauw GJ, Murphy MB, Bollen EL, Buckley BM, Cobbe SM, Ford I, Gaw A, Hyland M, Jukema JW, Kamper AM, Macfarlane PW, Meinders AE, Norrie J, Packard CJ, Perry IJ, Stott DJ, Sweeney BJ, Twomey C, Westendorp RG and Risk PsgPSoPitEa. Pravastatin in elderly individuals at risk of vascular disease (PROSPER): a randomised controlled trial. *Lancet*. 2002;360:1623-30.
79. Robin NC, Agoston Z, Biechele TL, James RG, Berndt JD and Moon RT. Simvastatin promotes adult hippocampal neurogenesis by enhancing Wnt/beta-catenin signaling. *Stem Cell Reports*. 2014;2:9-17.
80. Qiao LJ, Kang KL and Heo JS. Simvastatin promotes osteogenic differentiation of mouse embryonic stem cells via canonical Wnt/beta-catenin signaling. *Mol Cells*. 2011;32:437-44.
81. Esposito E, Rinaldi B, Mazzon E, Donniacuo M, Impellizzeri D, Paterniti I, Capuano A, Bramanti P and Cuzzocrea S. Anti-inflammatory effect of simvastatin in an experimental model of spinal cord trauma: involvement of PPAR-alpha. *Journal of neuroinflammation*. 2012;9:81.
82. Hu X, Song C, Fang M and Li C. Simvastatin inhibits the apoptosis of hippocampal cells in a mouse model of Alzheimer's disease. *Exp Ther Med*. 2018;15:1795-1802.

83. Park SH, Kim JH, Choi KH, Jang YJ, Bae SS, Choi BT and Shin HK. Hypercholesterolemia accelerates amyloid beta-induced cognitive deficits. *Int J Mol Med*. 2013;31:577-82.
84. Fassbender K, Simons M, Bergmann C, Stroick M, Lutjohann D, Keller P, Runz H, Kuhl S, Bertsch T, von Bergmann K, Hennerici M, Beyreuther K and Hartmann T. Simvastatin strongly reduces levels of Alzheimer's disease beta -amyloid peptides Abeta 42 and Abeta 40 in vitro and in vivo. *Proceedings of the National Academy of Sciences of the United States of America*. 2001;98:5856-61.
85. Kennedy DJ, Chen Y, Huang W, Viterna J, Liu J, Westfall K, Tian J, Bartlett DJ, Tang WH, Xie Z, Shapiro JI and Silverstein RL. CD36 and Na/K-ATPase-alpha1 form a proinflammatory signaling loop in kidney. *Hypertension*. 2013;61:216-24.
86. Hartley CJ, Reddy AK, Madala S, Martin-McNulty B, Vergona R, Sullivan ME, Halks-Miller M, Taffet GE, Michael LH, Entman ML and Wang YX. Hemodynamic changes in apolipoprotein E-knockout mice. *Am J Physiol Heart Circ Physiol*. 2000;279:H2326-34.
87. Xue J, Schmidt SV, Sander J, Draffehn A, Krebs W, Quester I, De Nardo D, Gohel TD, Emde M, Schmidleithner L, Ganesan H, Nino-Castro A, Mallmann MR, Labzin L, Theis H, Kraut M, Beyer M, Latz E, Freeman TC, Ulas T and Schultze JL. Transcriptome-based network analysis reveals a spectrum model of human macrophage activation. *Immunity*. 2014;40:274-88.
88. Peet C, Ivetic A, Bromage DI and Shah AM. Cardiac monocytes and macrophages after myocardial infarction. *Cardiovasc Res*. 2020;116:1101-1112.
89. Nie P, Li D, Hu L, Jin S, Yu Y, Cai Z, Shao Q, Shen J, Yi J, Xiao H, Shen L and He B. Atorvastatin improves plaque stability in ApoE-knockout mice by regulating chemokines and chemokine receptors. *PLoS One*. 2014;9:e97009.
90. Bea F, Blessing E, Bennett B, Levitz M, Wallace EP and Rosenfeld ME. Simvastatin promotes atherosclerotic plaque stability in apoE-deficient mice independently of lipid lowering. *Arteriosclerosis, thrombosis, and vascular biology*. 2002;22:1832-7.

Figure legends

Figure 1: ***Schematic overview illustrating experimental setup.*** **(A)** Blood pressure (BP) and memory function were tested in 4- and 12-months old ApoE$^{-/-}$ and WT mice simultaneously. At termination, immune status in blood and brain was assessed using flow cytometry, ELISA and qPCR. Synaptic marker expression was determined by Western blotting (WB) and qPCR. This approach aimed at characterizing aging in the ApoE$^{-/-}$ model in respect to plasma cholesterol levels, BP, systemic and neuro-inflammation as well as memory performance. **(B)** 12-months old ApoE$^{-/-}$ mice (associated with chronic hypercholesterolemia, increased BP, augmented systemic and neuro-inflammation and memory deficits) were subjected to 8-weeks cholesterol-lowering therapy (i.e. simvastatin), BP-lowering therapy (i.e. hydralazine) or a combination of both. BP was assessed longitudinally to monitor the effect of the different treatment regimens on BP. Memory function was assessed at 14 months of age. At termination, plasma cholesterol levels were determined by ELISA and systemic and neuroinflammation were assessed by ELISA, qPCR, WB and immunofluorescence to characterize the effects of the different treatment regimens on the different signatures we identified to be altered in this model (i.e. plasma cholesterol, BP, inflammatory status and memory function).

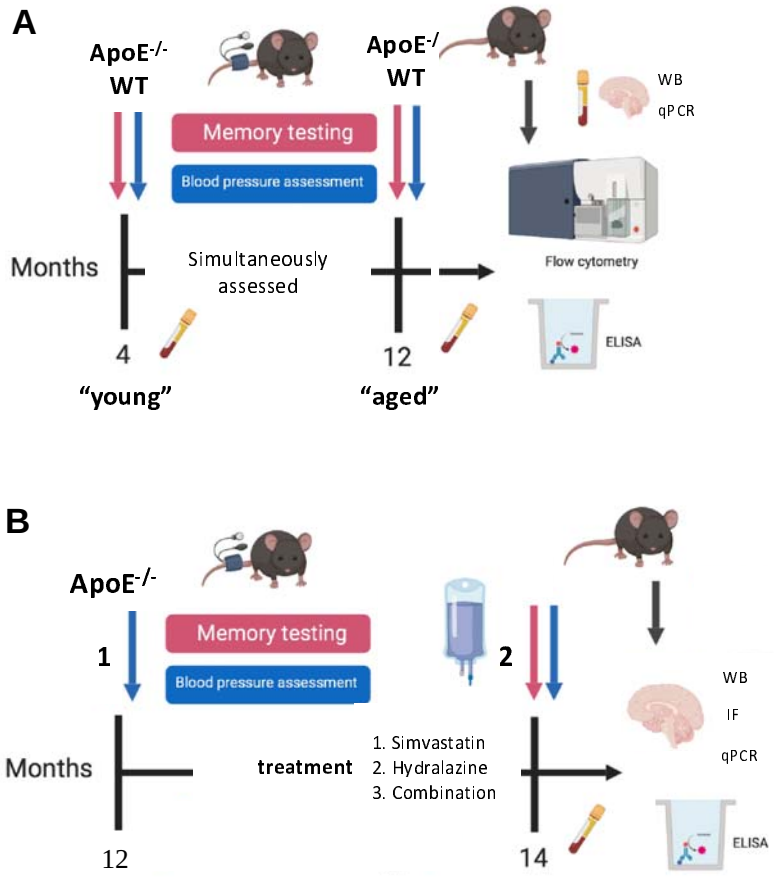

Figure 2: ***Chronic hypercholesterolemia impairs memory function.*** **(A)** Schematic illustration of novel object recognition task with 24-h delay interval. Recognition index (RI) describing hippocampus-dependent long-term memory function in young and aged WT and ApoE$^{-/-}$ mice (N=10 per group; some animals were excluded due to total object exploration times below 20s). The pink dotted line indicates the point where the animal has no preference for either object. **(B)** Schematic illustration of an object placement test with a 5 min delay interval. RI describing spatial short-term memory function in young and aged WT and ApoE$^{-/-}$ mice (N=10 per group; some animals were excluded due to total object exploration times below 20s). The pink dotted line indicates the point where the animal has no preference for either object. **(C)** Western blot analysis displaying unchanged pre- and post-synaptic protein (SNAP-25 and PSD-95) expression levels in whole brain tissue lysates of young and aged ApoE$^{-/-}$ mice (N=4 for young and N=5 for aged ApoE$^{-/-}$). **(D)** Brain region-specific mRNA expression analysis revealing reduced PSD-95 expression levels in aged ApoE$^{-/-}$ mice (N=4 for young cortex and N=5 for young hippocampus and aged cortex and hippocampus). N denotes number of independent biological replicates. In **A-D**, * denotes $P \leq 0.05$ relative to young control of same genotype, & denotes $P \leq 0.05$ relative to WT aged after two-way ANOVA followed by Sidak *post hoc* testing.

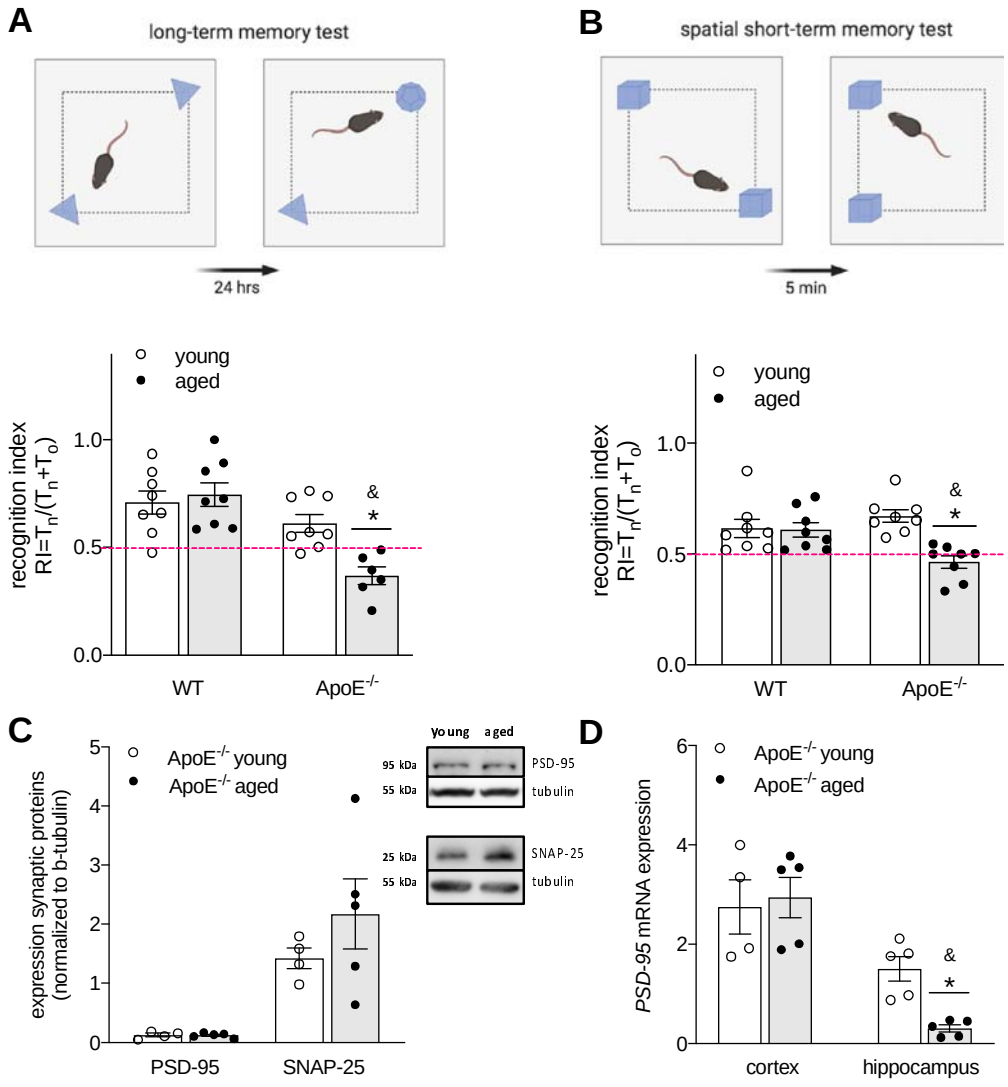

Figure 3: ***Immune system activation leads to leukocyte infiltration into the brain of aged ApoE$^{-/-}$ mice.*** **(A)** Percentage of circulating pro-inflammatory Ly6Chi monocytes determined by flow cytometry of young and aged ApoE$^{-/-}$ mice and representative images showing typical dot plots. **(B)** Plasma levels of pro-inflammatory IL12/23 and **(C)** IL17 of young and aged ApoE$^{-/-}$ mice determined by ELISA (N=10 per group; some samples failed to return a signal and were excluded from analysis). **(D)** Percentage of Ly6Chi monocytes in brain tissue of young and aged ApoE$^{-/-}$ mice analyzed by flow cytometry and representative dot plots (N=10 per group; some samples were excluded from analysis due to heavy myelin contamination). **(E)** Percentage of CD3+ T-cells in brain tissue of young and aged ApoE$^{-/-}$ mice analyzed by flow cytometry and representative dot plots (N=10 per group; some samples were excluded from analysis due to heavy myelin contamination). **(F)** Percentage of circulating pro-inflammatory Ly6Chi monocytes in young and aged WT mice (N=10 per group) compared to ApoE$^{-/-}$ mice determined by flow cytometry and representative images showing dot plots for WT mice. **(G)** Percentage of Ly6Chi monocytes in brain tissue of young and aged WT mice (N=10 per group) compared to ApoE$^{-/-}$ mice analyzed by flow cytometry and representative images showing dot plots for WT mice. N denotes number of independent biological replicates. In **A-E,** * denotes $P \leq 0.05$ for single, unpaired comparisons; in **F-G**, * denotes $P \leq 0.05$ relative to young control of same genotype, & denotes $P \leq 0.05$ relative to WT aged, and + denotes $P \leq 0.05$ relative to WT young after two-way ANOVA followed by Sidak *post hoc* testing.

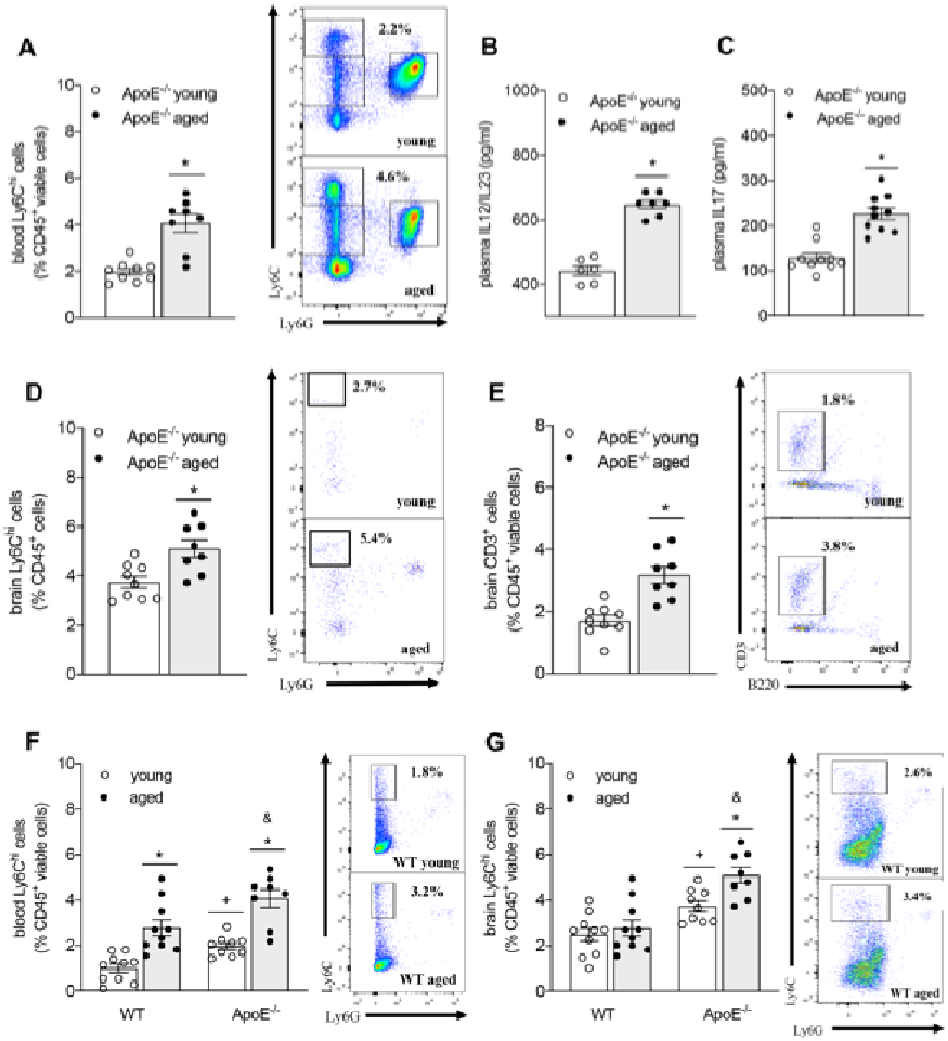

Figure 4: ***Simvastatin treatment attenuates systemic and neuro-inflammation in aged ApoE$^{-/-}$ mice.*** **(A)** Effect of cholesterol- and BP-lowering treatment (hydralazine – green circle, simvastatin – pink circles, combination – orange circles) on plasma levels of pro-inflammatory IL12/23 and **(B)** IL17 determined by ELISA (N=10 per group and N=8 for aged + combination treatment; some samples failed to return a signal and were excluded from analysis). **(C)** Effect of cholesterol- and BP-lowering treatment on CD68 mRNA expression in whole brain extracts of aged ApoE$^{-/-}$ mice (N=5 per group). **(D)** Effect of cholesterol- and BP-lowering treatment on the number of CD68+ Iba1+ cells in the CA1 region of the hippocampus of aged ApoE$^{-/-}$ mice (N=3 for young and aged + combination treatment; N=4 for aged control and simvastatin treatment; N=5 for hydralazine treatment; the two hemispheres were counted separately. **(E)** Effect of cholesterol- and BP-lowering treatment on the CD68+ Iba1+ cells in the DG region of the hippocampus of aged ApoE$^{-/-}$ mice (N=3 for young and aged + combination treatment; N=4 for aged control and simvastatin treatment; N=5 for hydralazine treatment; the two hemispheres were counted separately). **(F)** Effect of cholesterol- and BP-lowering treatment on the total Iba1+ cell count in the CA1 region of the hippocampus of aged ApoE$^{-/-}$ mice (N=3 for young and aged + combination treatment; N=4 for aged control and simvastatin treatment; N=5 for hydralazine treatment; the two hemispheres were counted separately except for a sample in the aged + hydralazine group where one hippocampus region was not analyzable). **(G)** Effect of cholesterol- and BP-lowering treatment on CD86 mRNA expression in the hippocampus of aged ApoE$^{-/-}$ mice (N=5 per group). **(H)** Effect of cholesterol- and BP-lowering treatment on CD3 protein expression in whole brain lysates of aged ApoE$^{-/-}$ mice (N=4 for hydralazine- and combination-treated groups and N=5 for control and simvastatin-treated groups). Inset showing representative protein expression pattern. N denotes number of independent biological replicates. In **A-C** and **G-H,** * denotes P ≤ 0.05 relative to young control, & denotes P ≤ 0.05 relative to aged control after one-way ANOVA followed by Tukey's *post hoc* testing. In **F**, * denotes P ≤ 0.05 relative to young control, & denotes P ≤ 0.05 relative to aged control after Kruskal-Wallis followed by Dunn's *post hoc* testing.

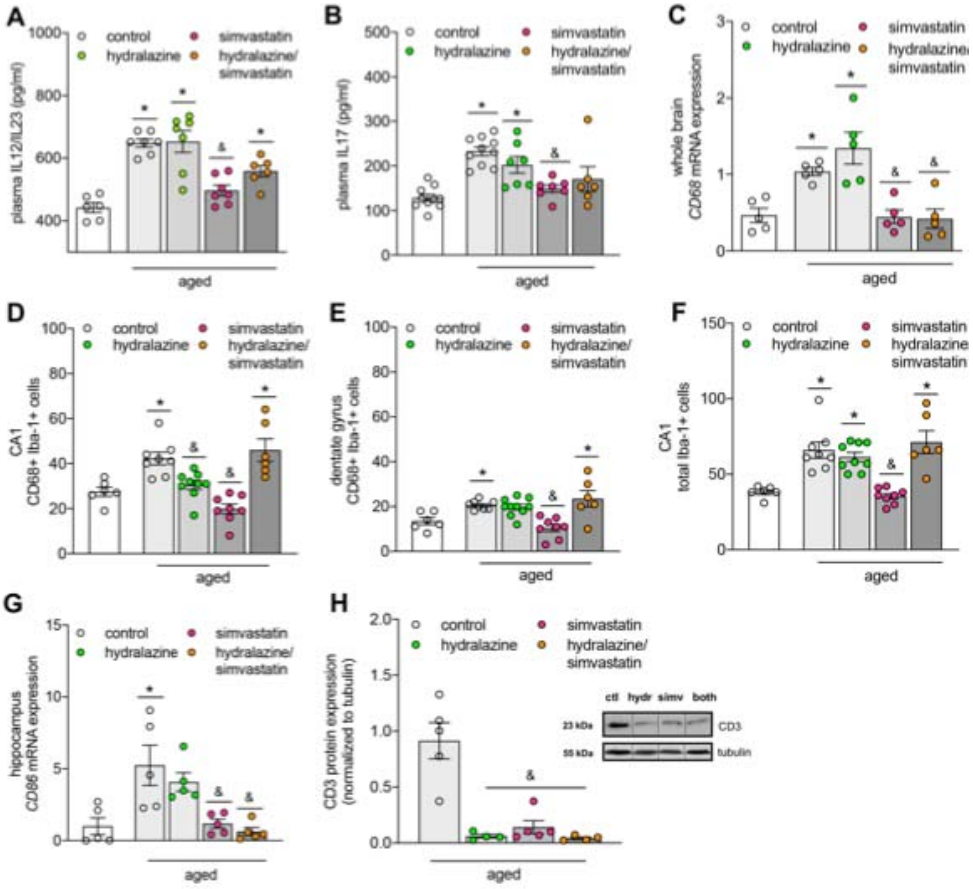

Figure 5: *Simvastatin mitigates impaired memory function of aged ApoE$^{-/-}$ mice.* (A) Quantification of open field test assessing mobility in aged ApoE$^{-/-}$ mice treated with hydralazine (green circles), simvastatin (pink circles) and a combination of both (orange circles) in comparison to young and aged control mice (open circles). (N=10 per group; some animals were excluded due to total mobile times below 20s). Representative images showing (*i*) young control, (*ii*) aged control, (*iii*) aged + hydralazine, (*iv*) aged + simvastatin, and (*v*) aged + hydralazine/simvastatin. **(B)** Effect of lipid- and BP lowering treatment on long-term memory function, and on **(C)** spatial long-term memory function. (N=10 per group; some animals were excluded due to total object exploration times below 20s). The pink dotted line indicates the point where the animal has no preference for either object. **(D)** Effect of lipid- and BP lowering treatment on hippocampal BDNF mRNA expression (N=5 for young, aged and hydralazine-treated groups; N=4 for simvastatin- and combination-treated groups). **(E)** Representative images of BDNF (green) and NeuN (red) immune staining showing a hippocampal CA region as illustrated in (*i*) HE-stained coronal brain section of an aged ApoE$^{-/-}$ mouse: (*ii*) aged control, (*iii*) aged + hydralazine, (*iv*) aged + simvastatin, and (*v*) aged + combined treatment. Quantification of BDNF-NeuN ratio comparing young and aged ApoE$^{-/-}$ mice with treatment groups (N=3 for young and aged + combination treatment; N=4 for aged control and simvastatin treatment; N=5 for hydralazine treatment). N denotes number of independent biological replicates. In **A**, * denotes $P \leq 0.05$ relative to young control, & denotes $P \leq 0.05$ relative to aged control after Kruskal-Wallis followed by Dunn's *post hoc* testing. In **B-D**, * denotes $P \leq 0.05$ relative to young control, & denotes $P \leq 0.05$ relative to aged control after one-way ANOVA followed by Tukey's *post hoc* testing.

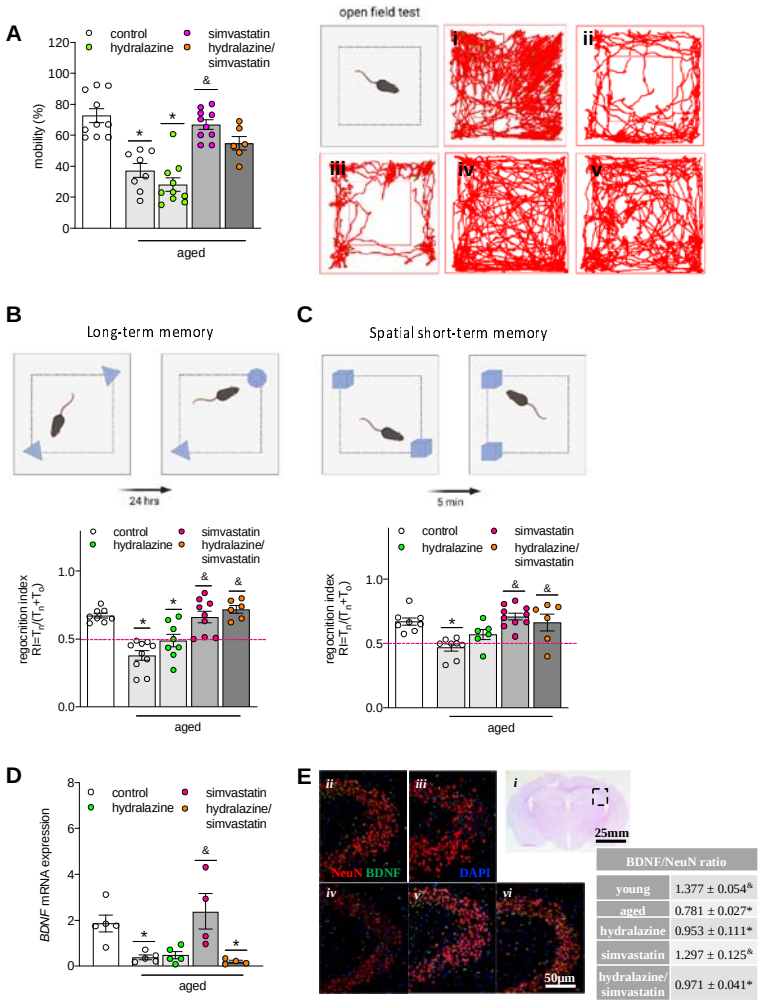

Figure 6: ***Simvastatin reduces monocyte activation***. **(A)** Degree of myeloid cell activation in response to hydralazine determined by flow cytometric assessment of CD69 surface expression (expressed in fold change compared to control) in human monocytic THP-1 cells and PMA-treated monocyte-derived macrophages compared to human primary monocytes and monocyte-derived macrophages (N=3 per group). Representative histograms showing the typical CD69+ cell distribution. **(B)** Degree of myeloid cell activation in response to simvastatin determined by flow cytometric assessment of CD69 surface expression (expressed in fold change compared to control) in human primary monocytes and monocyte-derived macrophages (N=3 per group). Representative histograms showing the typical CD69+ cell distribution. **(C)** Effect of hydralazine and simvastatin on LPS-induced TNF-α protein expression in human monocytic THP-1 cells determined by WB (N=4 in control and combination-treated groups; N=5 in LPS control, hydralazine- and simvastatin-treated groups). **(D)** Effect of hydralazine and simvastatin on LPS-induced intracellular IL6 expression in human monocytic THP-1 cells determined by flow cytometry (N=5 per group)**.** Representative dot plot showing the typical IL6+ cell distribution. **(E)** Effect of hydralazine and simvastatin on intracellular IL6 expression in human monocytic THP-1 cells determined by flow cytometry (N=5 per group)**.** Representative dot plot showing the typical IL6+ cell distribution. **(F)** Effect of hydralazine and simvastatin on LPS-mediated TNF-α and **(G)** IL6 release in murine bone marrow-derived macrophages assessed by ELISA (N=4 for untreated control and hydralazine-treated cells, N=8 for LPS-treated control and simvastatin-treated cells). N denotes number of independent biological replicates. In **A,** * denotes $P \leq 0.05$ relative to respective control for unpaired t-test; in **C-F** * denotes $P \leq 0.05$ relative to control, & denotes $P \leq 0.05$ relative to LPS-treated control after one-way ANOVA followed by Tukey's *post hoc* testing.

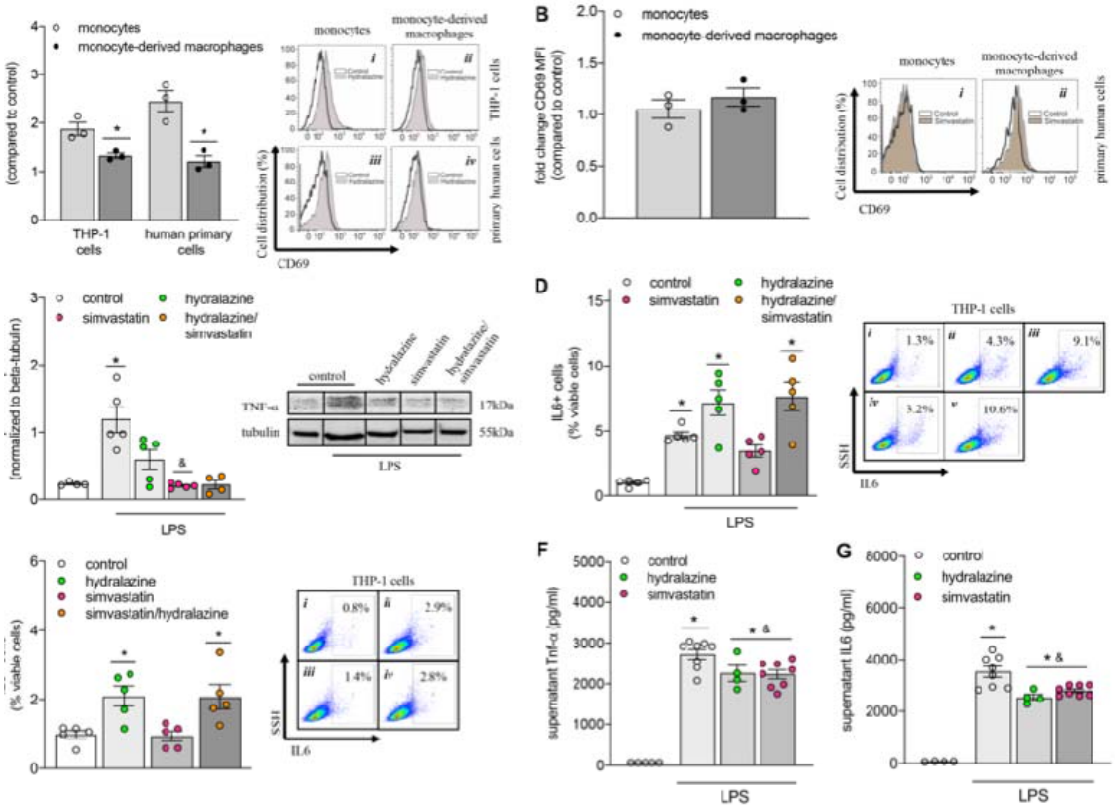
monocytes
monocyte-derived macrophages
(compared to control)
THP-1 cells
human primary cells
Cell distribution (%)
CD69
THP-1 cells
primary human cells
B
fold change CD69 MFI (compared to control)
control
simvastatin
hydralazine
hydralazine/ simvastatin
(normalized to beta-tubulin)
LPS
TNF-α
tubulin
17kDa
55kDa
IL6+ cells (% viable cells)
(% viable cells)
simvastatin/hydralazine
SSH
IL6
supernatant Tnf-α (pg/ml)
supernatant IL6 (pg/ml)

895

SUPPLEMENTAL MATERIAL

Simvastatin Therapy Attenuates Memory Deficits that Associate to Brain Monocyte Infiltration in Chronic Hypercholesterolemic ApoE$^{-/-}$ Mice

Nicholas Don-Doncow[a,b], Frank Matthes[a,b], Hana Matuskova[a,b,c,d], Sara Rattik[e], Lotte Vanherle[a,b], Sine Kragh Petersen[f], Anetta Härtlova[f] & Anja Meissner[a,b,d]

[a] Department of Experimental Medical Sciences, Lund University, Sweden

[b] Wallenberg Centre for Molecular Medicine, Lund University, Sweden

[c] Department of Neurology, University Hospital Bonn, Germany

[d] German Center for Neurodegenerative Diseases, Bonn, Germany

[e] Department of Clinical Science, Lund University, Sweden

[f] Department of Microbiology and Immunology, Wallenberg Centre for Molecular and Translational Medicine, University of Gothenburg, Sweden

Correspondence to: Anja Meissner; Klinikgatan 32, SE-22184 Lund, Sweden; anja.meissner@med.lu.se; +46 (0)46 22 20641

METHODS

Western Blotting: For protein isolation, tissue lysates were prepared using RIPA buffer containing 10mM Tris (pH 8.0), 1mM EDTA, 1% Triton-X, 0.1% sodium-deoxycholate, 0.1% SDS, 140mM NaCl and 25µg/ml protease inhibitor cocktail. Lysates underwent five freeze-thaw cycles using liquid nitrogen. The resulting lysates were centrifuged for 30 min at 15,000g and 4ºC to remove insoluble material. Protein concentration was determined by PIERCE BCA protein assay (Fisher Scientific, Sweden). Western blotting was carried out according to standard protocols. Briefly, samples were heated for 10 min at 95ºC in sample buffer (2.0ml 1M Tris-HCl, pH 6.8, 2% SDS, 10% glycerol, 1% 14.7 M β-mercaptoethanol 12.5mM EDTA, 0.02% bromophenol blue). Proteins were then separated on 12% Bis-acrylamid mini gels and transferred onto PVDF membranes (Biorad, Sweden). The membranes were blocked for 60 min in 1% bovine serum albumin (in phosphate-buffered saline containing 1% Tween 20 (PBST); 137mM NaCl, 2.7mM KCl, 10mM Na_2HPO_4, 1.76mM K_2HPO_4; pH 7.4) and sequentially incubated with the primary and secondary antibodies. An antibody-specific dilution for the primary antibodies (see list below), and 1:40,000 for the HRP-labeled secondary antibody (BioNordika, Sweden) were utilized. All antibodies were diluted in 1% bovine serum albumin or 5% milk in PBST. A standard chemiluminescence procedure (ECL Plus) was used to visualize protein binding. The developed membranes were evaluated densitometrically using Image Lab 6.0.1 (Biorad, Sweden).

Antibody target	host	Supplier (catalogue #)	Antibody dilution
CD3	rabbit	Abcam (ab5690)	1:1000
Beta-tubulin	mouse	Sigma Aldrich (T4026)	1:3000
TNF-alpha	rabbit	Abcam (ab6671)	1:1000
SNAP-25	rabbit	Abcam (ab109105)	1:5000
PSD-95	rabbit	Abcam (ab76115)	1:2000

Quantitative real-time PCR (qPCR): RNA was isolated from brain tissue (N=5per group) using a Trizol® method. As per instructions using a "High Capacity Reverse Transcriptase" kit (AB Bioscience, Stockholm, Sweden), 500ng of total RNA was reverse transcribed with random hexamer primers. The resulting cDNA was diluted to a final volume of 250µl and subsequently used as a template for qPCR reactions. qPCR was performed in triplicates using *Power* SYBR® Green PCR Master Mix (Life Technology, Sweden) according to the manufacturer's instructions. Each reaction comprised 2ng cDNA, 3ul master mix and 0.2uM final concentration of each primer. Cycling and detection were carried out using a CFX Connect™ Real-Time PCR Detection System and data quantified using Sequence CFX Manager™ Software (Biorad, Sweden). qPCR was performed

for a total of 40 cycles (95°C 15 sec, 60°C 60 sec) followed by a dissociation stage. All data were normalized to species specific housekeeping genes L14 (mouse) and GPI (human) and quantification was carried out via the absolute method using standard curves generated from pooled cDNA representative of each sample to be analyzed.

Target	**Primer sequence (mouse)**
L14	F: 5'-GGCTTTAGTGGATGGACCCT-3’ R: 5'-ATTGATATCCGCCTTCTCCC-3'
TBP	F: 5’-GAAGCTGCGGTACAATTCCAG-3’ R: 5’-CCCCTTGTACCCTTCACCAAT-3’
IL12	F: 5'-CATCTGGTTCAGTGCTTTGATCT-3’ R: 5'-ACCCGTGAGTTATTCCATGAGT-3'
MCP-1	F: 5'-CACGACATGCACGTTTGACT-3’ R: 5'-GGCGCAGATAAGGCTTCACA-3'
TNF-a	F: 5'-GTTTGCAGTCTCTCAAGCTTTT-3’ R: 5'-CCGATTTGAGCAATCGTTT-3'
IL6	F: 5'-AGGAGTGATACCAGCTTTAGTCC-3’ R: 5'-CCGAGCAGGTCAGAACAAAGG-3'
iNOS	F: 5'-GGC AGC CTG TGA GAC CTT TG-3' R: 5'-GCA TTG GAA GTG AAG CGT TTC-3'
CXCl2	F: 5'-GTCCCAGACATCAGGGAGTAA-3’ R: 5'-TCGGATACTTCAGCGTCAGGA-3'
IL23	F: 5'-GACCCACAAGGACTCAAGGAC-3’ R: 5'-ATGGGGCTATCAGGGAGTAGAG-3'
Arg-1	F: 5'-TTGCGAGACGTAGACCCTGG-3’ R: 5'-CAAAGCTCAGGTGAATCGGC-3'
CD68	F: 5'-TGTCTGATCTTGCTAGGACCG-3’ R: 5'-GAGAGTAACGGCCTTTTTGTGA-3'
CD86	F: 5'-AGAACTTACGGAAGCACCCAC-3’ R: 5'-CTGCCAAAATACTACCAGCTCAC-3'
PSD-95	F: 5'-ACCGCTACCAAGATGAAGACAC-3’ R: 5'-CTCCTCATACTCCATCTCCCC-3'
BDNF	F: 5'-TGCAGGGGCATAGACAAAAGG-3’ R: 5'-CTTATGAATCGCCAGCCAATTCTC-3'

Target	Primer sequence (human)
GPI	F: 5'-AGG CTG CTG CCA CAT AAG GT-3' R: 5'-CCA AGG CTC CAA GCA TGA AT-3'
INF-γ	F: 5'-ACTGACTTGAATGTCCAACGCA-3' R: 5'-ATCTGACTCCTTTTTCGCTTCC-3'
IL-6	F: 5'-TGC GTC CGT AGT TTC CTT CT-3' R: 5'-GCC TCA GAC ATC TCC AGT CC-3'

Histology and Immunofluorescence: Coronal brain sections (10 µm thickness) were incubated with antibody against NeuN, BDNF, IBA-1 and CD68. After several washes, sections were incubated with secondary Alexa Fluor-coupled antibodies (Life Technologies, Sweden) at room temperature. Sections were then mounted in aqueous DAPI-containing media (DapiMount, Life Technologies, Sweden). The specificity of the immune staining was verified by omission of the primary antibody and processed as above, which abolished the fluorescence signal.

Antibody target	host	Supplier (catalogue #)	Antibody dilution
BDNF	rabbit	Abcam (ab6201)	1:250
NeuN	mouse	Abcam (ab104224)	1:250
Iba-1	rabbit	WAKO (019-19741)	1:1000
CD68 (ED-1)	rat	Invitrogen (MA5-16654)	1:500

List of antibodies used for immunohistochemistry.

Quantification of immune-histological experiments: For quantification of hippocampal NeuN+ cells, three regions of interest (ROI) in the cortex and three brain sections representing the hippocampus were selected. The number of NeuN+ cells in the pyramidal layer of the CA3 region, of the CA1 region and the granule cell layer of the dentate gyrus as well as in the cortical ROIs was determined using ImageJ software (ImageJ 1.48v, http://imagej.nih.gov/ij). First, a binary image was generated from the original images. To measure the total number of stained cells the analyze particle feature was chosen and the threshold was maintained at the level that is automatically provided by the program, no size filter was applied. BDNF immune staining in the same three brain regions was quantified, and by dividing the obtained value by the corresponding number of NeuN+ cells the ratio of BDNF per NeuN+ cell was obtained for the respective area. Staining was analyzed in three images per area and mouse. For each experimental group $N=5$. Values are expressed as mean +/- SEM.

***ELISA*:** TNF-α and IL6 protein levels in cell supernatant and plasma IL12/23 and IL17 protein levels were determined using DuoSet Elisa (R&D systems) as per manufacturer's instruction.

Fluorescence activated cell sorting – in vitro experiments: Cells were collected and washed with PBS before samples were incubated with primary antibodies for 30 minutes at 4ºC. After centrifugation, the supernatant was decanted, washed, and re-suspended in FACS buffer (PBS + 2% FBS + 2mM EDTA; pH 7.4). Jurkat cells were additionally incubated with Fc-block. Data acquisition was carried out in a BD LSR Fortessa cytometer using FacsDiva software Vision 8.0 (BD Biosciences). Data analysis was performed with FlowJo software (version 10, TreeStar Inc., Ashland, OR, USA). Cells were plotted on forward versus side scatter and single cells were gated on FSC-A versus FSC-H linearity.

SUPPLEMENTAL FIGURES

SUPPLEMENTAL FIGURE 1: Systolic blood pressure (BP_{sys}) of 12- and 14-months old $ApoE^{-/-}$ mice before and after treatment with BP- and cholesterol-lowering drugs (hydralazine, simvastatin and combination treatment). Values expressed in mean ± SEM*; N denotes number of independent biological replicates; N=10 for aged control, aged + hydralazine and aged + simvastatin treatment; N=8 for aged + combination treatment; * denotes P ≤ 0.05 relative 12 months (pre-treatment) after Two-way repeated measure ANOVA and Sidak post hoc testing.*

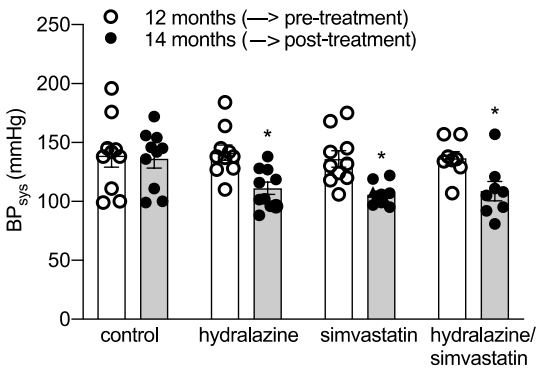

SUPPLEMENTAL FIGURE 2: Total number of CD68+ Iba1+ cells in the cortex of 14-months old $ApoE^{-/-}$ mice compared to 4-months old $ApoE^{-/-}$ mice, and the effect of BP- and cholesterol-lowering therapy (hydralazine – green circle, simvastatin – pink circles, combination – orange circles). Values expressed in mean ± SEM*; N denotes number of independent biological replicates; N=3 for young and aged + combination treatment; N=4 for aged control and simvastatin treatment; N=5 for hydralazine treatment; * denotes P ≤ 0.05 relative to young control, & denotes P ≤ 0.05 relative to aged control after Kruskal Wallis followed by Dunn's post hoc testing.*

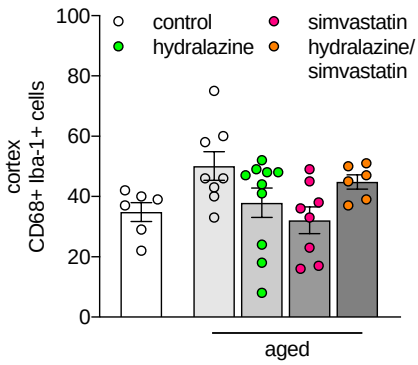

SUPPLEMENTAL FIGURE 3: Total number of Iba1+ cells in **(A)** the dentate gyrus and **(B)** the cortex of 14-months old $ApoE^{-/-}$ mice compared to 4-months old $ApoE^{-/-}$ mice, and the effect of BP- and cholesterol-lowering

therapy (hydralazine – green circle, simvastatin – pink circles, combination – orange circles). N denotes number of independent biological replicates. In **A** and **B**, values expressed in mean ± SEM; *N=3 for young and aged + combination treatment; N=4 for aged control and simvastatin treatment; N=5 for hydralazine treatment; * denotes P ≤ 0.05 relative to young control, & denotes P ≤ 0.05 relative to aged control after Kruskal Wallis followed by Dunn's post hoc testing.*

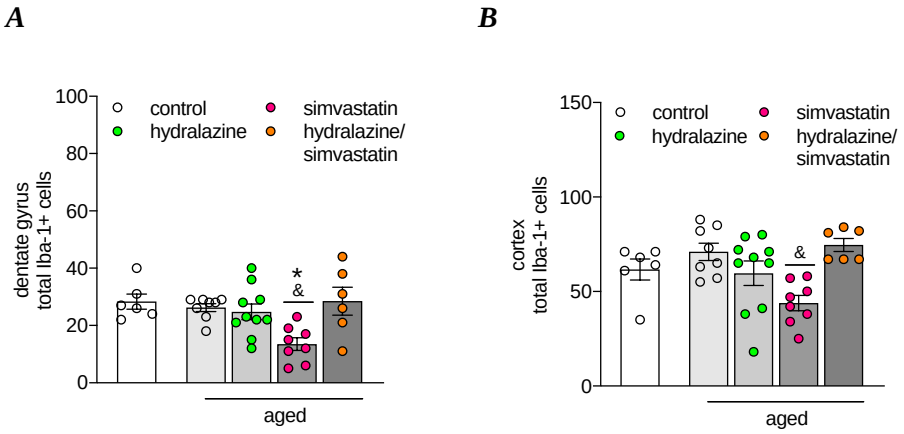

SUPPLEMENTAL FIGURE 4: Flow cytometric assessment of hydralazine effects on CD3 expression in (**A**) monocytic THP-1 cells, (**B**) PMA-differentiated THP-1 macrophages, (**C**) primary human blood monocytes, and (**D**) primary human monocyte-derived macrophages. **(E)** Representative histograms showing hydralazine responses in THP-1 cells and human primary cells. N denotes number of independent biological replicates. In **A-D**, values are expressed in mean ± SEM; *N=3 per group. * denotes P ≤ 0.05 compared to respective control after unpaired t-test.*

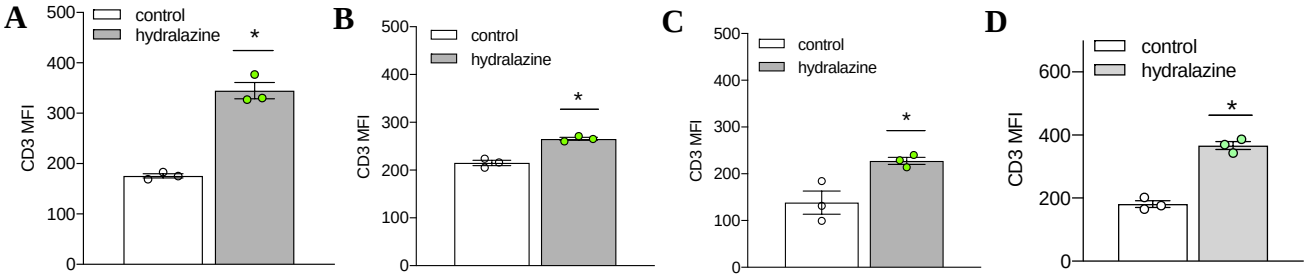

E

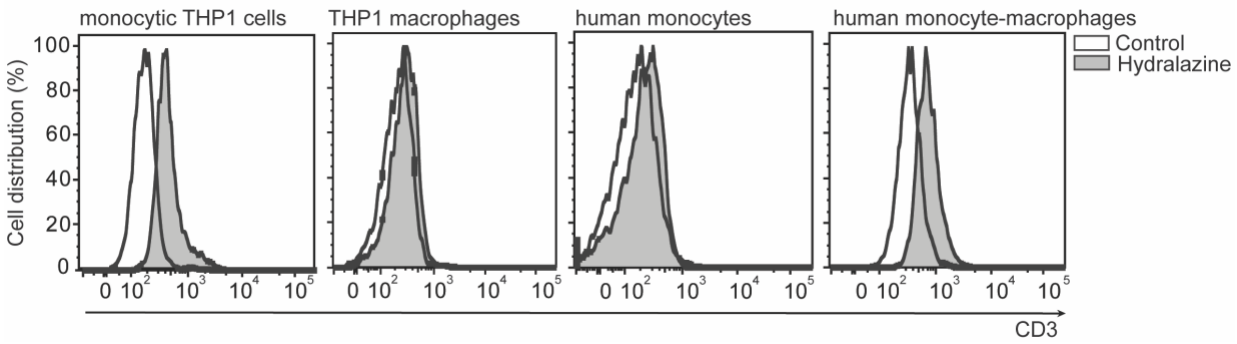

SUPPLEMENTAL FIGURE 5: mRNA expression levels of IL6 prior and post activation with 1µM LPS in human PMA-pre-treated monocytic cells (THP-1), and the effect of BP- and cholesterol-lowering therapy (hydralazine – green circle, simvastatin – pink circles). Values expressed in mean ± SEM; *N denotes number of independent biological replicates; N=6 for control groups and N=3 for treated groups; * denotes P ≤ 0.05 relative to untreated control, & denotes P ≤ 0.05 relative to LPS control after Kruskal-Wallis followed by Dunn's post hoc testing.*

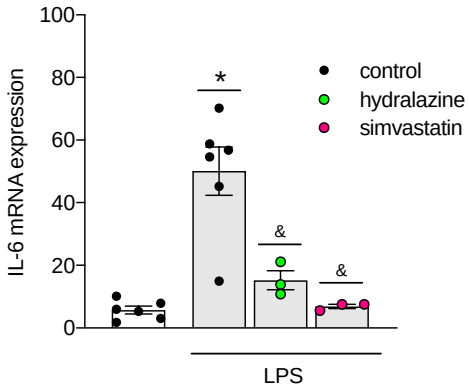

SUPPLEMENTAL FIGURE 6: Flow cytometry analysis of (**A**) CD86 and (**B**) CD80 responses to LPS, simvastatin and hydralazine in murine bone marrow-derived macrophages, and the effect of BP- and cholesterol-lowering therapy (hydralazine – green circle, simvastatin – pink circles). N denotes number of independent biological replicates. In **A-B**, values expressed in mean ± SEM;*; N=3 per group; * denotes P ≤ 0.05 relative to untreated control, & denotes P ≤ 0.05 relative to LPS control after one-way ANOVA followed by Tukey's post hoc testing.*

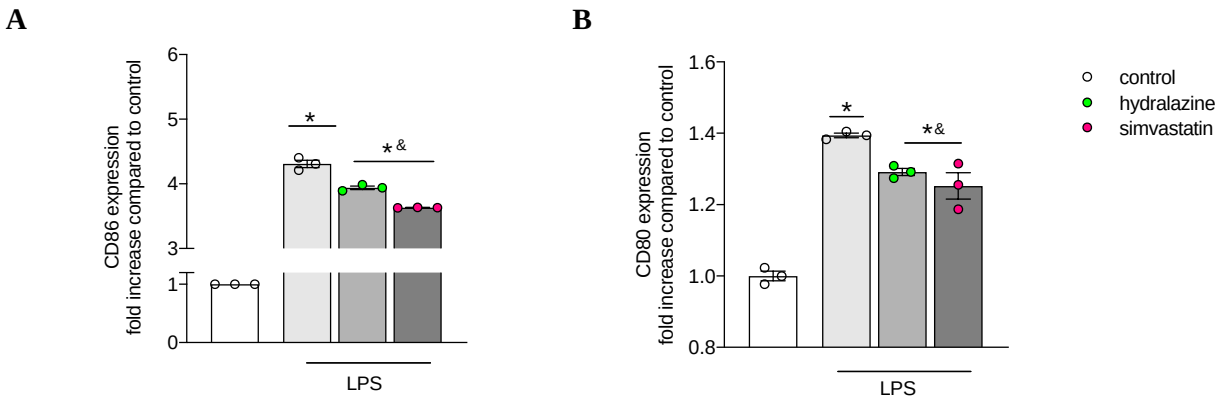

SUPPLEMENTAL FIGURE 7: Flow cytometry analysis of CD14+ CD16+ cells in (**A**) monocytic THP-1 cells and (**B**) PMA-differentiated THP-1 cells following LPS activation and treatment with simvastatin, hydralazine or a combination of both (hydralazine – green circle, simvastatin – pink circles, combination – orange circles). N denotes number of independent biological replicates. In **A**, values expressed in mean ± SEM; *N=5 per group; * denotes P ≤ 0.05 relative to untreated control, & denotes P ≤ 0.05 relative to LPS control after one-way ANOVA followed by Tukey's post hoc testing.* In **B**, values expressed in mean ± SEM; *N=4 per group; * denotes P ≤ 0.05 relative to LPS-treated control after one-way ANOVA followed by Tukey's post hoc testing.*

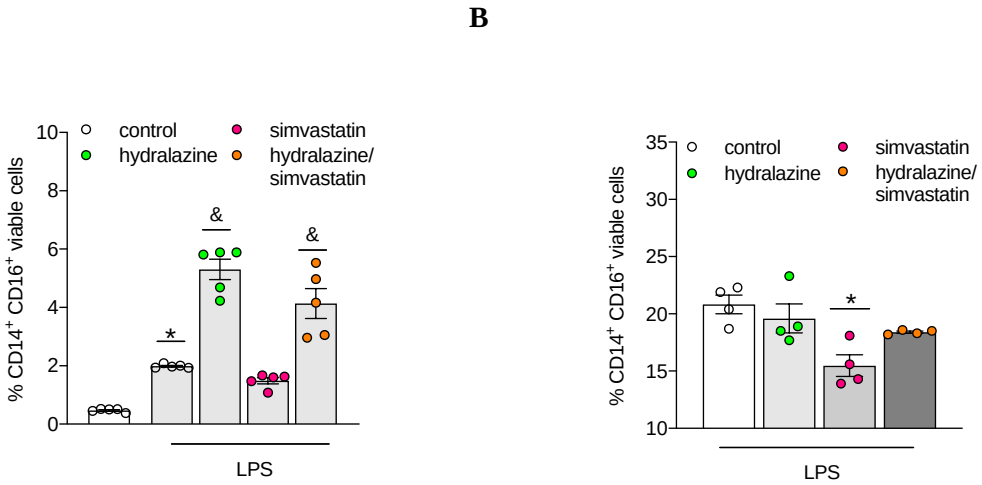

SUPPLEMENTAL FIGURE 8: Flow cytometry analysis of Jurkat cells showing percentage of $CD69^{+}$ cells following LPS, simvastatin or hydralazine treatment (hydralazine – green circle, simvastatin – pink circles, combination – orange circles). Values expressed in mean ± SEM. N denotes number of independent biological replicates. *N=4-5 per group. Significance tested with Kruskal-Wallis followed by Dunn's post hoc testing.*

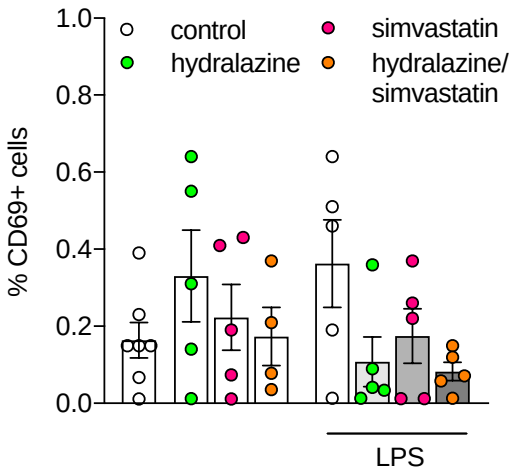
1.0
0.8
0.6
0.4
0.2
0.0
% CD69+ cells
control
hydralazine
simvastatin
hydralazine/
simvastatin
LPS

SUPPLEMENTAL TABLES

SUPPLEMENTAL TABLE 1: Behavioral parameters of WT and ApoE$^{-/-}$ mice obtained in novel object recognition tasks with 5 min or 24hrs delay interval. Recognition indices (RI) as the main index of retention were calculated by the time spent investigating the novel object relative to the total object investigation [RI = $T_{Novel}/(T_{Novel} + T_{Familiar})$]. An RI=0.5 indicates that the animal has no preference for neither familiar nor novel object. *Values expressed as mean+/- SEM; N denotes number of independent biological replicates; N=10 per group.* Mice with total object exploration times ($T_{Novel} + T_{Familiar}$) below 20s were excluded from the analysis. *Statistical differences were assessed with non-parametric Mann Whitney tests for single unpaired comparisons.*

	recognition index **5 min delay**	**P value** *compared to young control*	**recognition index** **24 hrs delay**	**P value** *compared to young control*
WT young (4 months)	0.71 ± 0.05		0.57 ± 0.05	
WT aged (12 months)	0.74 ± 0.06	0.6403	0.58 ± 0.05	0.7974
ApoE$^{-/-}$ young (4 months)	0.76 ± 0.02		0.63 ± 0.02	
ApoE$^{-/-}$ aged (12 months)	0.73 ± 0.03	0.4584	0.36 ± 0.04	0.0009

SUPPLEMENTAL TABLE 2: Brain mRNA expression of inflammatory markers in 12-months old ApoE$^{-/-}$ versus 12-months old WT mice. Values are expressed as fold change compared to aged WT mice. *N=5 per group; N denotes number of independent biological replicates.*

gene	**Fold change (ApoE$^{-/-}$ vs. WT)**
MCP-1	5.673
CXCL2	4.924
GFAP	1.969
CD68	2.927
IL6	5.507

SUPPLEMENTAL TABLE 3: Hemodynamic data and plasma cholesterol levels of ApoE$^{-/-}$ mice. Systolic BP (BP sys) and heart rate (HR) were measured in conscious mice using tail cuff plethysmography. Heart – body weight (BW) ratio calculated from animal weight (g) and respective heart weight (mg). Cholesterol levels were determined in plasma obtained from anaesthetized mice. *Values are expressed as mean +/- SEM. N denotes number of independent biological replicates; N=10 per group and N=8 for aged ApoE$^{-/-}$ treated with*

*hydralazine/simvastatin combined; * denotes P ≤ 0.05 relative to young control, & denotes P ≤ 0.05 relative to aged group after one-way ANOVA followed by Tukey's post hoc testing.*

	ApoE$^{-/-}$ young (4 months)	**ApoE$^{-/-}$ aged (14 months)**	**ApoE$^{-/-}$ aged + hydralazine**	**ApoE$^{-/-}$ aged + simvastatin**	**ApoE$^{-/-}$ aged + hydralazine/simvastatin**
BP_{sys} (mmHg)	107.3 ± 3.1	136.9 ± 5.8*	110.1 ± 1.9$^{\&}$	105.4 ± 1.6$^{\&}$	112.6 ± 1.5$^{\&}$
HR (bpm)	491.1 ± 9.7	569.9 ± 8.6*	514.3 ± 10.9	512.2 ± 18.3	520.0 ± 12.9
Cholesterol (mg/L)	99.8 ± 4.3	184.7 ± 5.3*	227.9 ± 13.6*	108.7 ± 2.6*$^{\&}$	187.4 ± 13.4*
Heart BW ratio	4.59 ± 0.06	5.53 ± 0.21*	5.27 ± 0.16*	4.67 ± 0.56$^{\&}$	5.31 ± 0.22*

SUPPLEMENTAL TABLE 4: Morphological quantification of immune-stained Iba+ cells in hippocampus regions (CA1 and dentate gyrus) and cortex from all experimental groups. The cells were classified into three activation state groups based on morphology where *Ramified* (resting state) denotes Iba-1+ cells with a small cell body and extensive branched processes, *Intermediate* denotes Iba-1+ cells with enlarged cell body and reduced branches not longer than twice the cell body length and *Round* (active state) denotes Iba-1+ cells with round cell body without visible branches. *Values are expressed as mean +/- SEM; N=3 for young and aged + combination treatment; N=4 for aged control and simvastatin treatment; N=5 for hydralazine treatment. N denotes number of independent biological replicates. For CA1 and DG, * denotes P ≤ 0.05 relative to young control, & denotes P ≤ 0.05 relative to aged control after one-way ANOVA followed by Tukey's post hoc testing; for cortex, * denotes P ≤ 0.05 relative to young control, & denotes P ≤ 0.05 relative to aged control after Kruskal Wallis followed by Dunn's post hoc testing.*

	ApoE$^{-/-}$ young (4 months)	**ApoE$^{-/-}$ aged (14 months)**	**ApoE$^{-/-}$ aged + hydralazine**	**ApoE$^{-/-}$ aged + simvastatin**	**ApoE$^{-/-}$ aged + hydralazine/simvastatin**
Hippocampus – CA1					
Ramified	95.08 ± 1.25	86.24 ± 2.18	91.08 ± 1.53	72.69 ± 3.55$^{*\&}$	85.01 ± 1.76*
Intermediate	4.92 ± 1.25	13.18 ± 2.27	8.25 ± 1.44	24.88 ± 3.26$^{*\&}$	13.18 ± 2.17
Activated	0	0.58 ± 0.39	0.66 ± 0.35	2.43 ± 0.75*	1.82 ± 0.47
Hippocampus – DG					
Ramified	90.97 ± 1.65	73.04 ± 4.53*	81.27 ± 2.69	66.51 ± 3.27*	59.25 ± 6.12*
Intermediate	9.03 ±1.64	25.61 ± 4.69*	16.31 ± 2.73	28.38 ± 2.18*	22.13 ± 3.86
Activated	0	1.36 ± 0.66	2.42 ± 0.71	5.11 ± 1.84	18.61 ± 5.98$^{*\&}$
Cortex					
Ramified	93.10 ± 0.59	85.30 ± 1.88	88.08 ± 2.14	66.39 ± 4.30$^{*\&}$	80.51 ± 2.14*
Intermediate	6.90 ± 0.59	13.70 ± 2.12	10.28 ± 1.80	30.51 ± 4.18$^{*\&}$	15.17 ± 1.87
Activated	0	0.99 ± 0.32	1.64 ± 0.63	3.10 ± 1.00	4.32 ± 0.79*

SUPPLEMENTAL TABLE 5: Quantification of immune stained NeuN+ and BDNF+ cells in hippocampus regions (CA3, CA1 region and dentate gyrus) and cortex from all experimental groups. *Values are expressed as mean +/- SEM; N=3 for young and aged + combination treatment; N=4 for aged control and simvastatin treatment; N=5 for hydralazine treatment. N denotes number of independent biological replicates. * denotes P ≤ 0.05 relative to young control, & denotes P ≤ 0.05 relative to aged group after one-way ANOVA followed by Tukey's post hoc testing.*

	ApoE$^{-/-}$ young (4 months)	**ApoE$^{-/-}$ aged (14 months)**	**ApoE$^{-/-}$ aged + hydralazine**	**ApoE$^{-/-}$ aged + simvastatin**	**ApoE$^{-/-}$ aged + hydralazine/simvastatin**
hippocampus					
NeuN	1078.2 ± 59.8$^{\&}$	558.5 ± 55.8*	723.3 ± 69.8	797.5 ± 35.8*$^{\&}$	807.3 ± 50.1*$^{\&}$
BDNF	1484.0 ± 96.5$^{\&}$	438.5 ± 53.5*	675.0 ± 73.9	935.6 ± 37.7*$^{\&}$	751.0 ± 67.3
NeuN/BDNF ratio	1.377 ± 0.054$^{\&}$	0.781 ± 0.027*	0.953 ± 0.111*	1.297 ± 0.125$^{\&}$	0.971 ± 0.041*
cortex					
NeuN	768.0 ± 55.5	698.8 ± 55.9	940.8 ± 81.5	782.0 ± 39.3	939.0 ±50.2
BDNF	1650.0 ± 141.4	594.8 ± 68.0*	1266.0 ± 105.2$^{\&}$	1139.0 ± 171.9$^{\&}$	1151.0 ± 182.8$^{\&}$
NeuN/BDNF ratio	2.142 ± 0.032	0.845 ± 0.035*	1.364 ± 0.121	1.481 ± 0.265	1.213 ± 0.125

SUPPLEMENTAL TABLE 6: Flow cytometry analysis (percentages) of THP-1 cells, primary monocytes and monocyte-derived macrophages treated with hydralazine or simvastatin. *For each experimental group N=3. N denotes number of independent biological replicates. * denotes P ≤ 0.05 after one-way ANOVA followed by Tukey's post hoc testing.*

	treatment	**% CD3+ cells**	**% CD69+ cells**
THP-1 monocytes	vehicle	4.23 ± 0.20	3.58 ± 0.09
	10uM hydralazine	11.87 ± 0.43*	18.27 ± 0.49*
THP-1 macrophages	vehicle	6.23 ± 0.26	5.13 ± 0.18
	10uM hydralazine	12.30 ± 0.36*	15.70 ± 0.66*
Human primary monocytes	vehicle	2.56 ± 0.23	1.70 ± 0.13
	10uM hydralazine	4.50 ± 0.72*	6.48 ± 0.38*
	1uM simvastatin	2.80 ± 0.35	2.30 ± 0.36
Human primary monocyte-derived macrophages	vehicle	6.83 ± 0.33	8.07 ± 0.43
	10uM hydralazine	16.00 ± 1.16*	9.20 ± 0.51
	1uM simvastatin	8.73 ± 0.62	6.33 ± 0.32*

SUPPLEMENTAL TABLE 7: Antibody list for flow cytometry experiments**.**

Target	Host/species	Label/dye	clone	dilution	distributor
CD11b	Rat anti-mouse	PE-Texas Red	M1/70.15	1:100	Life Technology
CD3	Rat anti-mouse	eFluor450	17A2	1:100	eBioscience
CD45	Rat anti-mouse	AF700	30-F11	1:100	eBioscience
CD45R	Rat anti-mouse	AF488	RA3-6B2	1:100	BioTechne
Ly6C	Rat anti-mouse	PE-Cy7	HK1.4	1:100	eBioscience
Ly6G	Rat anti-mouse	APC	RB6-8C5	1:100	eBioscience
CD14	Anti-human	eFluor450	61D3	1:100	Life Technology
CD16	Anti-human	FITC	CB16	1:100	Life Technology
CD3	Anti-human	FITC	BW264/56	1:100	Miltenyi Biotec
CD69	Anti-human	APC	298614	1:100	Life Technology
Live/dead		Aqua-405		1:250	Life Technology

Western blot images (representative bands used for insets in main figures highlighted with red borders)

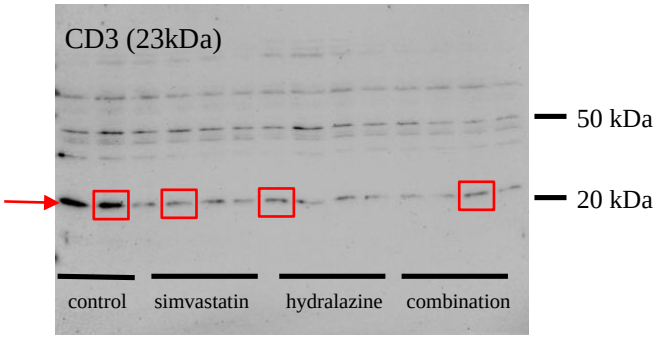

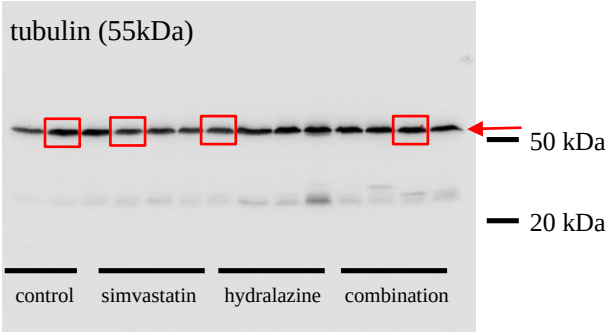

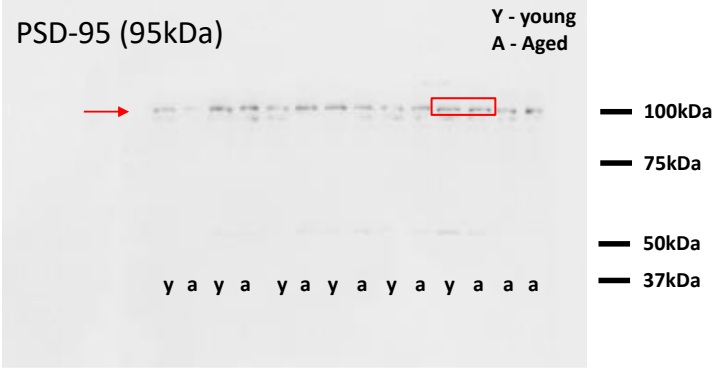

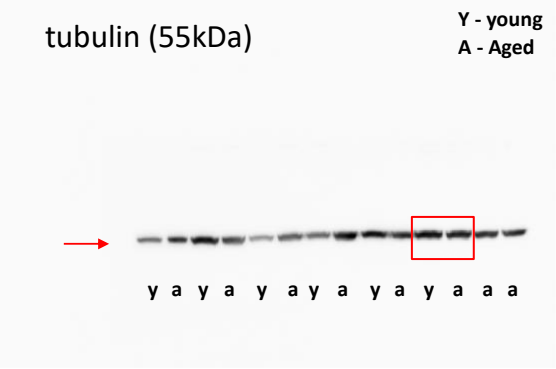

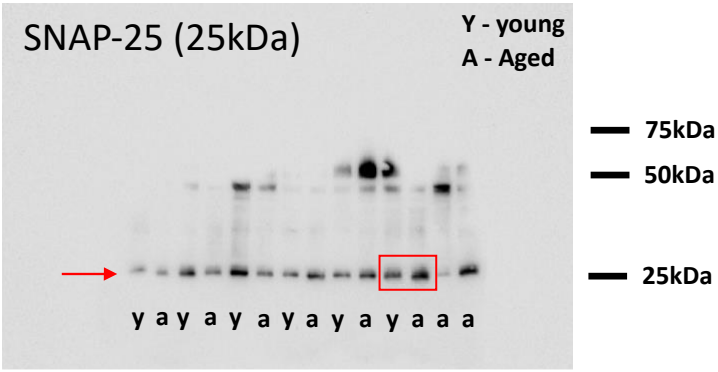

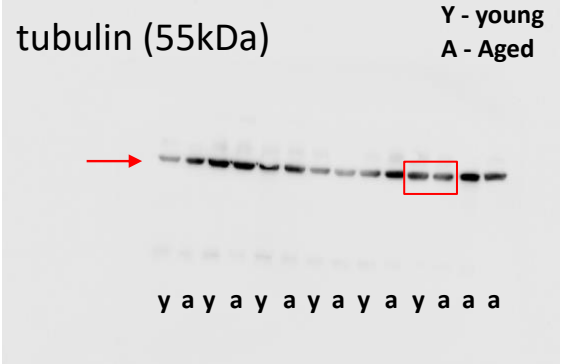

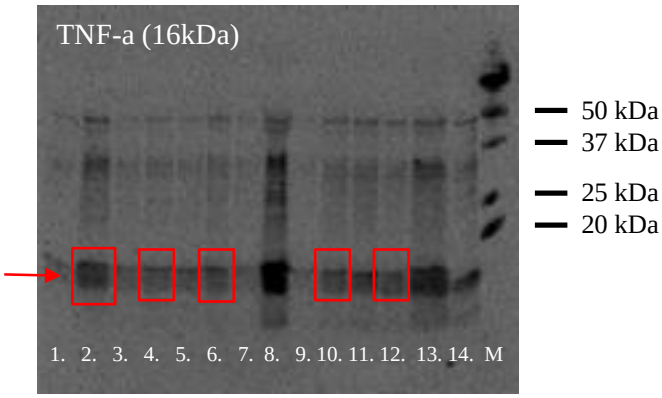

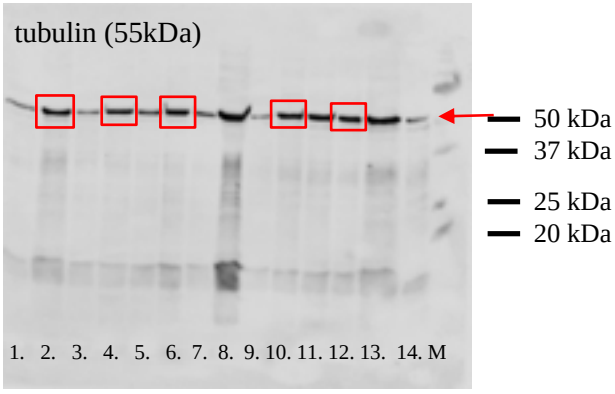

Control (4, 9, 14)

LPS (2, 8, 13)

LPS + hydralazine (3, 6, 11)

LPS + simvastatin (1, 7, 12)

LPS + combination (5, 10)

Bibliography

Meissner, A., Minnerup, J., Soria, G. and Planas, A. M. (2016) Structural and functional brain alterations in a murine model of Angiotensin II-induced hypertension. *Journal of neurochemistry*.

Meissner, A., Yang, J., Kroetsch, J. T. et al. (2012) Tumor necrosis factor-alpha-mediated downregulation of the cystic fibrosis transmembrane conductance regulator drives pathological sphingosine-1-phosphate signaling in a mouse model of heart failure. *Circulation*, **125,** 2739-2750.